
HYBRID MESSAGE PASSING ALGORITHM FOR DOWNLINK FDD MASSIVE MIMO-OFDM CHANNEL ESTIMATION

A PREPRINT

Yi Song, Chuanzong Zhang, Xinhua Lu, Fabio Saggese, Zhongyong Wang*

March 21, 2023

ABSTRACT

The design of message passing (MP) algorithms on factor graphs is an effective manner to implement channel estimation (CE) in wireless communication systems, which performance can be further improved by exploiting prior probability models that accurately match the channel characteristics. In this work, we study the CE problem in a downlink massive multiple-input multiple-output (MIMO) orthogonal frequency division multiplexing (OFDM) system. As the prior probability, we propose the Markov chain two-state Gaussian mixture with large variance differences (TSGM-LVD) model to exploit the structured sparsity in the angle-frequency domain of the channel. Existing single and combined MP rules cannot deal with the message computation of the proposed probability model. To overcome this issue, we present a general method to derive the hybrid message passing (HMP) rule, which allows the calculation of messages described by mixed linear and non-linear functions. Accordingly, we design the HMP-TSGM-LVD algorithm under the structured turbo framework (STF). Simulation results demonstrate that the proposed algorithm converges faster and obtains better and more stable performance than its counterparts. In particular, the gain of the proposed approach is maximum (3 dB) in the high signal-to-noise ratio regime, while benchmark approaches experience oscillating behavior due to the improper prior model characterization.

Keywords Massive MIMO, OFDM, FDD channel estimation, TSGM-LVD channel model, message passing.

1 Introduction

The combination of massive multiple-input multiple-output (MIMO) and orthogonal frequency-division multiplexing (OFDM) techniques can achieve huge performance gains in both spectrum and energy efficiency, playing an important role in 5th-generation (5G) applications [1, 2] and being a focused research area for 6th-generation (6G) technologies [3].

Massive MIMO-OFDM channel estimation (CE) has been one of the main focuses of academia and industry in recent years. Accurate channel state information (CSI) is essential for signal detection, resource allocation and beamforming. The CE problems in time division duplex (TDD) and frequency division duplex (FDD) are different. In TDD system, the CE problem can be solved by channel reciprocity property [4]. For now, most of the contemporary cellular networks have adopted the FDD protocol, which is more efficient for delay-sensitive and symmetric traffic applications [5]. However, in FDD massive MIMO-OFDM systems, it is challenging to improve the downlink CSI estimation accuracy without increasing the complexity of the algorithm and the pilot overhead.

Fortunately, massive MIMO-OFDM channels usually exhibit sparsity in the transform domain [6] due to the limited local scatterers in physical environments. Therefore, many compressed sensing (CS) based approaches have been

*Y. Song and Z. Wang are with the Department of Information Engineering, Zhengzhou University, 450001 Zhengzhou, China. Emails: songyizzu@gs.zzu.edu.cn, iezywang@zzu.edu.cn.

†C. Zhang and X. Lu are with the Research Center for Communications and Signal Processing, Nanyang Institute of Technology, 473000 Nanyang, China. Emails: ieczhang@gmail.com, ieluxinhua@sina.com.

‡F. Saggese is with the Department of Electronic Systems, Aalborg University, 9220 Aalborg, Denmark. Email: fasa@es.aau.dk.

proposed by exploiting sparsity information about the transform domain channel [7–11]. However, applying the above CS-based algorithms to the FDD downlink channel estimation problem straightforwardly is limited in massive MIMO-OFDM systems. Specifically, CS-based methods are susceptible to noise interference, while the observation matrix must satisfy the restricted isometry property (RIP).

Recently, message passing (MP) is receiving increasing attention from researchers due to its low computational complexity and high performance in terms of approximation [12–14]. A number of prior works investigated CSI estimation problem with MP [15–19]. In those works, MP tends to obtain better performance compared with traditional CS-based algorithms. More specifically, both the channel prior model which exploits the channel sparsity and message computation rules are critical aspects affecting the performance of MP algorithms employed for CE [16, 19]. Thus, in this work we focus on channel prior model construction and message computation rules selection.

1.1 Related Work

Researchers have developed many solutions focused on channel prior models [15, 19–21]. The authors in [15] proposed a Markov chain two-state Gaussian mixture (TSGM) prior model to exploit channel-tap sparsity and cluster structure for bit-interleaved coded orthogonal frequency division multiplexing (BICM-OFDM) system. [19] presented a Markov chain Bernoulli Gaussian (BG) prior model to design the structured turbo compressed sensing (STCS) algorithm by exploiting the clustered sparsity of the massive MIMO channel in the angle-frequency (AF) domain. [20] further extended the STCS algorithm to the massive MIMO-OFDM system. Employing the Markov chain BG prior model while proposing a structured turbo compressed sensing with frequency support (STCS-FS) algorithm, [20] achieved a considerably lower mean square error (MSE) performance compared with the CS-based algorithms with frequency support. Furthermore, [21] explored the massive MIMO-OFDM channel structured sparsity in the angle-delay domain, combined with Markov chain BG prior model to design structured turbo compressed sensing with delay support (STCS-DS) algorithm, which has the state-of-the-art performance in both complexity and convergence speed.

All of the above works [19–21] utilized the Markov chain BG model to characterize the massive MIMO-OFDM channels. The BG model assumes that the non-zero elements of the channel follow a Gaussian distribution while its small value elements are zero. On the contrary, in this work, we show that the elements with relatively small values of the channel in the AF domain are not zero but close to zero, coherently labelled as “*near-zero*” elements. Accordingly, the TSGM model [15] is more appropriate, making use of a Gaussian distribution for near-zero elements. However, TSGM assumes that the variances of the Gaussian distributions are the same. We find that the values of the non-zero elements within the AF domain channel vary significantly. According to the physical channel characteristics, it is more accurate to set different variances for the non-zero elements, while the near-zero elements’ Gaussian distributions have the same variance value. Based on the above considerations, we propose the two-state Gaussian mixture with large variance differences (TSGM-LVD) prior model to further characterize the near-zero elements and the large variation of the non-zero elements of the massive MIMO-OFDM channel. Furthermore, [15, 19–21] utilized the expectation maximization (EM) algorithm to update the hyperparameters of BG, TSGM, and the Markov chain. Differently from them, we treat TSGM-LVD hyperparameters as variables, updating them using MP algorithms. Indeed, updating the hyperparameters on the factor graph can simplify the derivation of the EM. Moreover, designing a suitable prior distribution for the hyperparameters can improve the algorithm convergence speed without increasing the complexity.

Constructing a prior model which accurately characterizes the physical channel is a prerequisite for achieving high accuracy CSI. Nevertheless, the challenge of designing a high-performance MP algorithm lies also in selecting the appropriate message calculation rules. In literature, three *single* calculation rules are commonly used to implement MP algorithms: belief propagation (BP), also known as sum-product algorithm [12], mean field (MF), also called variational message passing (VMP) [22], and expectation propagation (EP) [23]. These three rules have their specific application scenarios: BP rule is well-suited for discrete models with hard constraints and linear Gaussian models, while the performance deteriorates when applied to multi-variable product calculations or non-linear models [16]; MF rule is especially useful for the estimation of continuous parameters (e.g., noise variance), but it may exhibit poor performance when applied to multi-variable summation calculations or discrete variables with hard constraints [24]; EP rule can be regarded as an approximation of the BP rule, where beliefs are approximated by distributions in a specific exponential family [25]. In general, it is difficult to use a single rule to compute all the message calculations due to multiple types of variables and the complicated relationship among them. To address this issue, [14] proposed the *combined* BP-MF rule, used as a base for a considerable number of works [16, 17, 24, 25]. However, faced with *mixed linear and non-linear models*, i.e., in the presence of complicated factor nodes expressing joint product summation operations during message computation, the combined rule can not be applied directly; indeed, the aforementioned combined rule is constrained to use BP *or* MF at each node, not being able to deal with mixed models. Unfortunately, these mixed linear and non-linear models are common in practical communication systems.

Recently, [26] proposed a framework based on *constrained Bethe free energy* (BFE) minimization approach; BFE is used to derive, among others, a hybrid message passing (HMP) rule through the formulation of different constraints on system variables. The main advantage of the HMP rule is that enables the simultaneous use of different single message calculation rules at the same factor node, allowing the evaluation of messages in presence of mixed linear and non-linear probability models, overcoming the main limitation of single and combined rules. Based on [26], [27] applied the BFE minimization framework to solve the massive MIMO CE problem, implicitly applying HMP rule in the derivation of the algorithm. However, [26, 27] focus on the BFE framework and do not directly utilize an HMP approach; the main disadvantage is the need of reformulating and solving the constrained BFE minimization problem any time we deal with a new problem. This prevents the direct use of the HMP rule on the factor graph which is a more simpler and straightforward approach.

Differently from other works in literature, in this article, we propose a generalized formulation and derivation of the HMP rule that allows us to design MP algorithms omitting the BFE derivation process. Furthermore, we apply the proposed HMP rule derivation on the proposed two-state Gaussian mixture with large variance difference (TSGM-LVD) prior model, developing a structured turbo framework (STF) CE algorithm for downlink massive MIMO-OFDM scenario. A detailed list of contribution is given in the next subsection. We summarize the characteristics of various models and message calculation rules in Table 1; the proposed TSGM-LVD model using the HMP rule has clear advantages over the others, as we will demonstrate throughout the article.

Finally, we remark that the HMP rule studied in this article is different from most of the existing works related to HMP approaches [28–30]. The HMP mentioned in [28, 29] refers to approximation methods aiming to reduce the complexity of message computations, while [30] refers to the iterative exchange of messages between two modules performing different estimation processes. Instead, the HMP rule proposed in this article is a new method of message computation for factor graphs, being an evolved version of single and combined computation rules.

Table 1: Summary of related channel prior models and MP rules.

Prior model \ Rule	BG [21]	TSGM [15]	TSGM-LVD (proposed)
BP-EM [21]	Neglects the near-zero elements Parameters updated by EM	Neglects the variation of non-zero elements Parameters updated by EM	–
HMP [26]	Neglects the near-zero elements Parameters treated as variables	Neglects the variation of non-zero elements Parameters treated as variables	Consider channel full characteristics Parameters treated as variables

1.2 Main Contributions

The main contributions of this article can be summarized as follows: OFDM FDD downlink CE problem modeled as a TSGM-LVD.

- **Generalized hybrid message passing rule:** First, we propose a general formulation of the HMP rule and its derivation. In this way, we can apply the HMP rule to design MP algorithms directly on the factor graph and omit the BFE derivation process. Second, we innovatively divide the factor graph from the edge perspective. The above classification method enables the application of different message updating rules to different messages departing, effectively handling the problem of message computation for mixed linear and non-linear models. Third, we give new insight into the connection among the HMP rule, the single MP rules and the combined MP rule from the edge perspective.
- **TSGM-LVD probability model:** We study the AF domain channel characteristics of the massive MIMO-OFDM system and propose the TSGM-LVD probability model, which can fully exploit the clustered sparsity of AF domain channel. As a baseline, we utilize the two-state Gaussian mixture (TSGM) probability model to indicate the numerical characteristics of the non-zero and near-zero elements of the AF domain channel. On top of that, we propose the TSGM-LVD probability model to account for the large variation among non-zero elements' channel. Finally, we use the Markov chain formulation to represent the cluster sparsity of non-zero and near-zero elements within the AF domain channel.
- **Hybrid message passing algorithm for massive MIMO-OFDM CE:** Based on the TSGM-LVD probability model, we utilize the proposed HMP rule to design the AF domain CE algorithm for massive MIMO-OFDM system, yielding the HMP-TSGM-LVD algorithm, whose convergence can be well predicted by the state evolution (SE). Numerical examples show that the proposed HMP-TSGM-LVD algorithm exhibits the fastest convergence, and provides better normalized mean square error (NMSE) performance than the state-of-the-art STCS-FS algorithm [19–21] while maintaining the same complexity.

The rest of the article is organized as follows. In Section 2, we present the HMP rule, whose detailed derivation is given in the Appendix A. Then, we present the system model and the system factor graph in Section 3. In Section 4, we propose the HMP-TSGM-LVD channel estimation algorithm for massive MIMO-OFDM system. Simulation results are given in Section 5. Our conclusions are finally drawn in Section 6.

Notation: Boldface lowercase and uppercase letters denote vectors and matrices, respectively; superscripts $(\cdot)^T$ and $(\cdot)^H$ denote transposition and Hermitian transposition, respectively. $|\mathcal{I}|$ denotes the cardinality of a finite set \mathcal{I} , the relative complement of $\{i\}$ in \mathcal{I} is written as $\mathcal{I} \setminus i$. The expectation operator of a function $f(x)$ with respect to a probability density function (PDF) $g(x)$ is expressed as $\mathbb{E}[f(x)]_{g(x)} = \langle f(x) \rangle_{g(x)} = \int f(x)g(x)dx / \int g(x)dx$; $\text{Var}(x)_{g(x)} = \langle |x|^2 \rangle_{g(x)} - |\langle x \rangle_{g(x)}|^2$ stands for the variance. We denote that a variable x follows a complex Gaussian distribution with mean μ and variance v using $\mathcal{CN}(x; \mu, v)$. $\text{Ga}(\cdot; a, b)$ denotes a Gamma PDF with shape parameter a and rate parameter b . $\text{Beta}(\cdot; e, f)$ denotes a Beta PDF with two shape parameters e and f . The relation $f(x) = cg(x)$ for some positive constant c is written as $f(x) \propto g(x)$.

2 Hybrid Message Passing Rule

In this section, we introduce the combined BP-MF rule; based on this rule, we present a new approach to derive HMP rule [26] in a more general and intuitive way. Then, we propose a new approach to analyze the relationships between the HMP rule and single, combined BP-MF rules.

2.1 Combined BP-MF rule

Let $p(\mathbf{x})$ be an arbitrary PDF of a random vector $\mathbf{x} \triangleq (x_i | i \in \mathcal{I})^T$. We group all the factors represented by the set \mathcal{A} into two disjunctive sets: $\mathcal{A}_{\text{BP}} \cap \mathcal{A}_{\text{MF}} = \emptyset$ and $\mathcal{A}_{\text{BP}} \cup \mathcal{A}_{\text{MF}} = \mathcal{A}$. After the factorization, the PDF can be written as

$$p(\mathbf{x}) = \prod_{a \in \mathcal{A}} f_a(\mathbf{x}_a) = \prod_{b \in \mathcal{A}_{\text{BP}}} f_b(\mathbf{x}_b) \prod_{c \in \mathcal{A}_{\text{MF}}} f_c(\mathbf{x}_c), \quad (1)$$

where $\mathbf{x}_a, \mathbf{x}_b$ and \mathbf{x}_c denote the vector of the variables x_i that are arguments of the factor nodes f_a, f_b and f_c , respectively. Moreover, we define $\mathcal{N}(a) \subseteq \mathcal{I}$ to be the set of indices of all variables x_i that are arguments of factor node f_a . Correspondingly, $\mathcal{N}(i) \subseteq \mathcal{A}$ denotes the set of indices of all factor nodes f_a that depend on x_i . The parts of the factorization that correspond to $\prod_{b \in \mathcal{A}_{\text{BP}}} f_b(\mathbf{x}_b)$ and $\mathcal{I}_{\text{BP}} \triangleq \bigcup_{b \in \mathcal{A}_{\text{BP}}} \mathcal{N}(b)$ are referred to as ‘‘BP part’’; $\prod_{c \in \mathcal{A}_{\text{MF}}} f_c(\mathbf{x}_c)$ and $\mathcal{I}_{\text{MF}} \triangleq \bigcup_{c \in \mathcal{A}_{\text{MF}}} \mathcal{N}(c)$ are referred to as ‘‘MF part’’. The combined BP-MF rule [14, 25] is

$$m_{f_a \rightarrow x_i}^{\text{BP}}(x_i) = \int f_a(\mathbf{x}_a) \prod_{j \in \mathcal{N}(a) \setminus i} n_{x_j \rightarrow f_a}(x_j) dx_j, \forall a \in \mathcal{A}_{\text{BP}}, i \in \mathcal{N}(a), \quad (2)$$

$$m_{f_a \rightarrow x_i}^{\text{MF}}(x_i) = \exp \left\{ \langle \ln f_a(\mathbf{x}_a) \rangle_{\prod_{j \in \mathcal{N}(a) \setminus i} n_{x_j \rightarrow f_a}(x_j)} \right\}, \forall a \in \mathcal{A}_{\text{MF}}, i \in \mathcal{N}(a), \quad (3)$$

$$n_{x_i \rightarrow f_a}(x_i) \propto \prod_{b \in (\mathcal{A}_{\text{BP}} \cap \mathcal{N}(i)) \setminus a} m_{f_b \rightarrow x_i}^{\text{BP}}(x_i) \prod_{c \in (\mathcal{A}_{\text{MF}} \cap \mathcal{N}(i))} m_{f_c \rightarrow x_i}^{\text{MF}}(x_i), \forall i \in \mathcal{I}. \quad (4)$$

The sets of \mathcal{A}_{BP} and \mathcal{A}_{MF} with the combined BP-MF rule can only connect variables of the corresponding type \mathcal{I}_{BP} and \mathcal{I}_{MF} , respectively. Therefore, only one rule can be used at one specific factor node. However, there are some factor nodes expressing joint product and summation operations in the practical system, on which the calculation cannot be completed using the combined BP-MF rule directly.

2.2 Hybrid message passing rule

In this subsection we present the HMP rule from the edge perspective. The factor graphs consist of variable nodes $x_i, i \in \mathcal{I}$, factor nodes $f_a, a \in \mathcal{A}$, and edges $ai \in \mathcal{E}$ connected with f_a and x_i [12]. We group all edges \mathcal{E} into two sets as \mathcal{E}_{BP} and \mathcal{E}_{MF} , which satisfy $\mathcal{E}_{\text{BP}} \cap \mathcal{E}_{\text{MF}} = \emptyset$ and $\mathcal{E}_{\text{BP}} \cup \mathcal{E}_{\text{MF}} = \mathcal{E}$. All factor nodes are grouped into the set $\mathcal{A}_{\text{Hybrid}}$. We define $\mathcal{N}_{\text{BP}}(a)$ and $\mathcal{N}_{\text{MF}}(a)$ as the sets of variable indices connected to factor node f_a by BP edges and MF edges, respectively. Correspondingly, the sets of factor indices connected to x_i by BP edges and MF edges can be expressed as $\mathcal{N}_{\text{BP}}(i)$ and $\mathcal{N}_{\text{MF}}(i)$, respectively. Unlike the derivation given in [26], we have reformulated the HMP

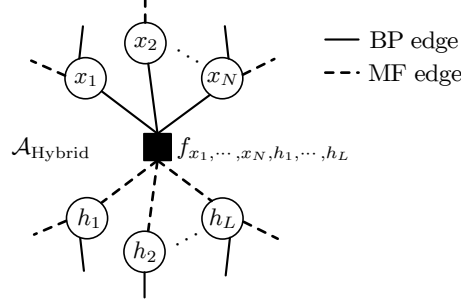


Figure 1: A partial factor graph representing the HMP rule.

rule to make it more intuitive and efficient. The HMP rule is

$$m_{f_a \rightarrow x_i}^{\text{BP}}(x_i) = \int \exp\left\{ \langle \ln f_a \rangle_{\prod_{j \in \mathcal{N}_{\text{MF}}(a)} b(h_j)} \right\} \prod_{k \in \mathcal{N}_{\text{BP}}(a) \setminus i} n_{x_k \rightarrow f_a}(x_k) dx_k, \forall ai \in \mathcal{E}_{\text{BP}}, \quad (5)$$

$$n_{x_i \rightarrow f_a}^{\text{BP}}(x_i) \propto \prod_{b \in \mathcal{N}_{\text{BP}}(i) \setminus a} m_{f_b \rightarrow x_i}^{\text{BP}}(x_i) \prod_{c \in \mathcal{N}_{\text{MF}}(i)} m_{f_c \rightarrow x_i}^{\text{MF}}(x_i), \forall ai \in \mathcal{E}_{\text{BP}}, \quad (6)$$

$$m_{f_a \rightarrow h_l}^{\text{MF}}(h_l) = \exp\left\{ \langle \ln f_a \rangle_{b(\mathcal{N}_{\text{BP}}(a))} \prod_{j \in \mathcal{N}_{\text{MF}}(a) \setminus l} b(h_j) \right\}, \forall al \in \mathcal{E}_{\text{MF}}, \quad (7)$$

$$b(\mathcal{N}_{\text{BP}}(a)) = \exp\left\{ \langle \ln f_a \rangle_{\prod_{j \in \mathcal{N}_{\text{MF}}(a)} b(h_j)} \right\} \prod_{k \in \mathcal{N}_{\text{BP}}(a)} n_{x_k \rightarrow f_a}(x_k), \quad (8)$$

$$n_{h_l \rightarrow f_a}^{\text{MF}}(h_l) = b(h_l) \propto \prod_{b \in \mathcal{N}_{\text{BP}}(l)} m_{f_b \rightarrow h_l}^{\text{BP}}(h_l) \prod_{c \in \mathcal{N}_{\text{MF}}(l)} m_{f_c \rightarrow h_l}^{\text{MF}}(h_l), \forall al \in \mathcal{E}_{\text{MF}}, \quad (9)$$

where $b(h_l)$ denotes the belief of the variable h_l . The factor nodes $\mathcal{A}_{\text{Hybrid}}$ are able to connect variable nodes through different types of edges \mathcal{E}_{BP} and \mathcal{E}_{MF} . In this way, HMP rule can implement two message calculation rules from the same factor node to the connected variable nodes by different edges. As shown in Fig. 1, we assume that $f_a \in \mathcal{A}_{\text{Hybrid}}$ ⁴, variables x_1, \dots, x_N are connected to f_a by BP edges; while variables h_1, \dots, h_L are connected to f_a by MF edges. Then, the messages from factor node f_a to $x_i, ai \in \mathcal{E}_{\text{BP}}$ are calculated by (5), meanwhile the messages from the same factor node f_a to $h_l, al \in \mathcal{E}_{\text{MF}}$ are computed using (7) and (8). The opposite direction of the messages, i.e., from $x_i, ai \in \mathcal{E}_{\text{BP}}$ and $h_l, al \in \mathcal{E}_{\text{MF}}$ to f_a , are calculated by (6) and (9), respectively.

We can analyze the relationships among the different rules from the perspective of the edge. i) If all the edges in a factor graph belong to \mathcal{E}_{BP} , then the factor graph uses the BP rule only. ii) Instead, if all the edges in a factor graph belong to \mathcal{E}_{MF} , then the factor graph uses the MF rule. iii) If a factor graph contains two types of factor nodes $\mathcal{A}_{\text{BP}}, \mathcal{A}_{\text{MF}}$ and only one type of edge exists surrounding each type of factor node, then the factor graph uses the combined BP-MF rule. iv) If there are two types of edges surrounding a factor node in a factor graph, then the factor graph uses the HMP rule. Besides, if all the edges connected between a certain $\mathcal{A}_{\text{Hybrid}}$ and its related variable nodes belong to \mathcal{E}_{BP} , then the HMP rule at this factor node degenerates into the BP rule. Consequently, if all edges connected between a certain $\mathcal{A}_{\text{Hybrid}}$ and its related variable nodes belong to \mathcal{E}_{MF} , then, the HMP rule at this factor node degenerates into the MF rule. Compared with single and combined rules, HMP is more flexible to design message passing algorithms and therefore more suitable for solving complicated variational inference problems.

3 System Model and Graph Representation

In this section, we present the system model of our inference problem and its factor graph representation. We consider a single-cell downlink massive MIMO-OFDM system consisting of a single base station (BS) equipped with N antennas, organized in a half-wavelength spacing uniform linear array (ULA), serving multiple single-antenna users. We assume that a resource grid of K subcarriers and T OFDM slots are available for communication in the scenario; it is further assumed that the channel coefficient of each subcarrier remains constant during the duration of T slots. In the resource grid, $P < K$ subcarriers and $M < T$ slots are assigned to transmit pilot symbols, and used to perform the CE. We denote the downlink channel as $\mathbf{h}_f^{(p)} \in \mathbb{C}^{N \times 1}$, where the subscript f represents the frequency domain of the vector,

⁴Here, we simplify the expression $f_a \triangleq f_{x_1, \dots, x_N, h_1, \dots, h_L}$.

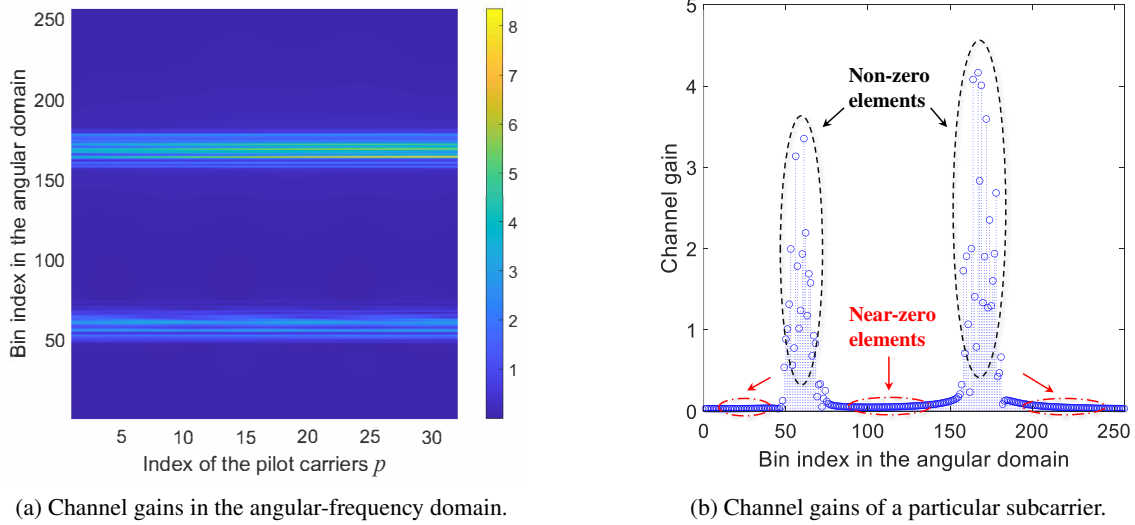


Figure 2: A realization of the spatial channel model in [31], with carrier frequency at 2 GHz, bandwidth 7.5 MHz and frequency interval 15 kHz. There are 512 subcarriers in total, and 32 of them are chosen as pilot subcarriers. The channel gains in subfigure (b) is $|\mathbf{h}_a^{(p)}|$.

while the superscript p indicates the p -th subcarrier, $1 \leq p \leq P$. In the remainder of this article, we use the 3GPP spatial channel model (SCM) to generate the massive MIMO-OFDM channel [31]. To estimate the downlink channel, the BS sends M training sequences $\mathbf{x}_m^{(p)} \in \mathbb{C}^{N \times 1}$, $1 \leq m \leq M$ in the reserved time slots. The matrix collecting all the training sequences is denoted as $\mathbf{X}^{(p)} = [\mathbf{x}_1^{(p)}, \dots, \mathbf{x}_M^{(p)}]^H \in \mathbb{C}^{M \times N}$. We assume that $\mathbf{X}^{(p)}$ is a Partial DFT Random Permutation (PDFTRP) pilot matrix [19], which is proved to outperform than an i.i.d. Gaussian pilot matrix [18]. Thus, the received signal at users $\mathbf{y}_f^{(p)}$ can be written as

$$\mathbf{y}_f^{(p)} = \mathbf{X}^{(p)} \mathbf{h}_f^{(p)} + \boldsymbol{\omega}_f^{(p)}, \quad 1 \leq p \leq P, \quad (10)$$

where $\boldsymbol{\omega}_f^{(p)} \sim \mathcal{CN}(\mathbf{0}, \sigma^2 \mathbf{I})$ denotes the additive white Gaussian noise (AWGN) with zero mean and variance σ^2 . Following the approaches of [6, 7, 11], we can transform the channel in the frequency domain $\mathbf{h}_f^{(p)}$ to the AF domain denoted by $\mathbf{h}_a^{(p)}$, as follows,

$$\mathbf{h}_a^{(p)} = \mathbf{B}^H \mathbf{h}_f^{(p)}, \quad 1 \leq p \leq P, \quad (11)$$

where \mathbf{B} is the unitary matrix representing the transformation of the virtual angular domain at the BS side. Due to the BS equipped with ULA antennas, \mathbf{B} is the discrete Fourier transform (DFT) matrix [6]. Substituting (11) into (10), and letting $\mathbf{A}^{(p)} = \mathbf{X}^{(p)} \mathbf{B}$, the received signal can be formulated as

$$\mathbf{y}_f^{(p)} = \mathbf{A}^{(p)} \mathbf{h}_a^{(p)} + \boldsymbol{\omega}_f^{(p)}, \quad 1 \leq p \leq P. \quad (12)$$

In this manner, we can focus on the estimation of the AF domain channel $\mathbf{h}_a^{(p)}$ based on the observed signal $\mathbf{y}_f^{(p)}$, $1 \leq p \leq P$. Due to the channel sparsity as shown in the following subsection, a channel prior model is an essential aspect to solve the problem, such as [19–21]. However, these existing methods use the Bernoulli-Gaussian as the probability model, which can not accurately characterize the channel. Therefore, we analyze the channel data and propose a more appropriate probability model in the next subsection.

3.1 Clustered-sparse Probability Model

The massive MIMO-OFDM channel exhibits clustered sparsity due to the scattering effect. Furthermore, the scatterers for different subchannels are quite similar [6]. Consequently, for a communication system with a much smaller bandwidth than the carrier frequency (as it is usually in the case of sub-6GHz communications), the subchannels $\{\mathbf{h}_a^{(p)}\}_{p=1}^P$ have a common support for sparsity [6], i.e.,

$$\text{supp}\{\mathbf{h}_a^{(1)}\} = \text{supp}\{\mathbf{h}_a^{(2)}\} = \dots = \text{supp}\{\mathbf{h}_a^{(P)}\}, \quad (13)$$

where $\text{supp}\{\mathbf{h}_a^{(p)}\}$ returns the positions of the non-zero entries of $\mathbf{h}_a^{(p)}$. In Fig. 2, we show a realization of the SCM urban macro scenario, generated by the parameters given in Table 3. Fig. 2(a) shows that channel elements are sparse and clustered together. The positions of the non-zero elements (light-coloured data) among the different subcarriers exhibit common support, verifying (13). In addition, as shown in Fig. 2(b), the smaller values of the channel elements are not zero, but are close to zero. In the remainder of the article, we call these elements as “near-zero” elements. Besides, we find that the values of the non-zero elements vary significantly with respect to the antenna index, while the values of the near-zero elements are approximately constant.

Taking into consideration the above channel characteristics, we develop the TSGM-LVD probability model, i.e., at the same subcarrier, the variance differs among the non-zero elements while it is the same among the near-zero elements. The probability model can be written as

$$p(h_{a,n}^{(p)}|s_n, v_S^{(p)}, v_{L,n}^{(p)}) = \delta(s_n) \mathcal{CN}(h_{a,n}^{(p)}; 0, v_S^{(p)-1}) + \delta(1-s_n) \mathcal{CN}(h_{a,n}^{(p)}; 0, v_{L,n}^{(p)-1}), \quad (14)$$

where $\delta(\cdot)$ denotes the Dirac delta function, $s_n \in \{0, 1\}$ is the hidden binary state indicating if the channel element is non-zero ($s_n = 1$) or near-zero ($s_n = 0$), $v_{L,n}^{(p)-1}$ denotes the variance of non-zero elements, and $v_S^{(p)-1}$ denotes the variance of near-zero elements. Then, the clustering effect of the non-zero elements can be modeled by a Markov chain as follows

$$p(\mathbf{s}) = p(s_1) \prod_{n=2}^N p(s_n|s_{n-1}), \quad (15)$$

with the transition and initial probabilities given by

$$p(s_n|s_{n-1}) = \begin{cases} (1-p_{10})^{(1-s_n)}(p_{10})^{(s_n)}, & s_{n-1} = 0; \\ (p_{01})^{(1-s_n)}(1-p_{01})^{(s_n)}, & s_{n-1} = 1. \end{cases} \quad (16)$$

and

$$p(s_1) = (p_{10})^{(s_1)}(1-p_{10})^{(1-s_1)}. \quad (17)$$

The Markov chain can be characterized by parameters $p_{10} \triangleq \Pr(s_n = 1|s_{n-1} = 0)$ and $p_{01} \triangleq \Pr(s_n = 0|s_{n-1} = 1)$ thoroughly. Here, p_{10} indicates the “spacing” between two clusters: on the one hand, a low value of p_{10} means that the transition probability from state 0 to state 1 is relatively small, i.e., there is a large probability that more near-zero elements will be clustered together. On the other hand, p_{01} reveal the size of the non-zero clusters: a low value of p_{01} indicates a high probability that more non-zero elements will be clustered together.

Prior works, such as [20, 21], initialize the probability in (17) using the sparsity variable $\lambda \triangleq \Pr(s_n = 1) = (1 + p_{01}/p_{10})^{-1}$, which indicates the average ratio of the non-zero elements in \mathbf{s} . When N tends to infinity, the initialization $\Pr(s_1 = 1) = (1 + p_{01}/p_{10})^{-1}$ is accurate [15]. However, in practice, when the BS has a limited number of antennas, initializing (17) as $\Pr(s_1 = 1) = p_{10}$ is more reasonable.

Regarding the initialization of the other variables, we use a different approach instead of the EM algorithm, e.g. [19–21]. The hyperprior of the precision terms $v_{L,n}^{(p)}$ and $v_S^{(p)}$ are assumed to be Gamma distributed⁵. In this way, the prior distribution of the precision terms are up to specific unknown parameters (see e.g., [16]). The distributions result

$$p(v_{L,n}^{(p)}) = \text{Ga}(v_{L,n}^{(p)}; \epsilon_n^{(p)}, \eta_n^{(p)}), \quad p(v_S^{(p)}) = \text{Ga}(v_S^{(p)}; \alpha^{(p)}, \beta^{(p)}), \quad (18)$$

where we control the different initial values of $v_{L,n}^{(p)}$ and $v_S^{(p)}$ by controlling the parameters $\epsilon_n^{(p)}, \eta_n^{(p)}$ and $\alpha^{(p)}, \beta^{(p)}$ of the Gamma distributions, respectively. Similarly, we also deem p_{01} and p_{10} as variables, generated by the Beta distributions as

$$p(p_{01}) = \text{Beta}(p_{01}; c, d), \quad p(p_{10}) = \text{Beta}(p_{10}; e, f), \quad (19)$$

where the parameters c, d and e, f determine the different initial values of p_{01} and p_{10} .

3.2 Structured Turbo Framework

To perform the CE, we use the structured Turbo framework (STF) [18], in conjunction with the channel probability model described in Section 3.1. The STF diagram consists in two modules [19], as shown in Fig. 3.

- *Module A* comprises a linear minimum mean square error (LMMSE) estimator, which utilize the measurement $\mathbf{y}_f^{(p)}$ as well as prior message $\mathcal{CN}(\mathbf{h}_a^{(p)}; \mathbf{h}_A^{\text{pri}(p)}, v_A^{\text{pri}(p)})$ from module B and output the *posteriori* message $\mathcal{CN}(\mathbf{h}_a^{(p)}; \mathbf{h}_A^{\text{post}(p)}, v_A^{\text{post}(p)})$;

⁵Note that, as in [32], we use the Gamma distribution for the parameter of precision, rather than for the variance [33].

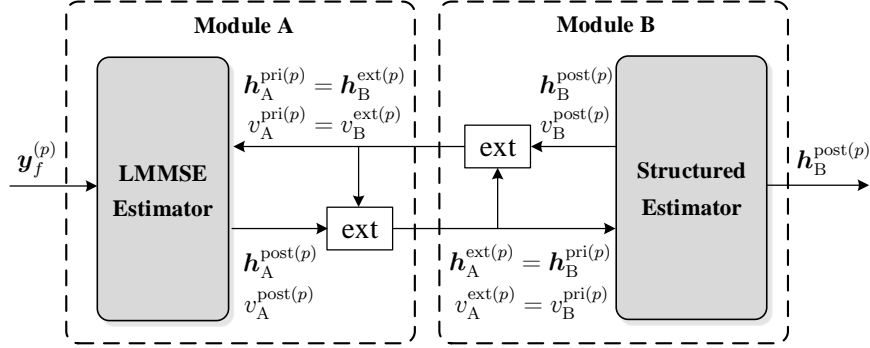


Figure 3: The block diagram of structured Turbo framework

- *Module B* includes a structured estimator, which can combine the channel probability model and prior message $\mathcal{CN}(\mathbf{h}_a^{(p)}; \mathbf{h}_B^{\text{pri}(p)}, v_B^{\text{pri}(p)})$ from module A to achieve better performance, and output $\mathbf{h}_B^{\text{post}(p)}$.

The two models compute the extrinsic messages⁶ $\mathbf{h}_A^{\text{ext}(p)}, v_A^{\text{ext}(p)}$ and $\mathbf{h}_B^{\text{ext}(p)}, v_B^{\text{ext}(p)}$ iteratively until the algorithm converges.

The STF utilized in this work is the same as [18–21, 34]. The parameters used in module A and the evaluation of the extrinsic messages between the two modules are detailed in [20, Algorithm 1]. The contributions of this article lie in the design of module B: the structured estimator uses the TSGM-LVD probability model to capture the channel sparsity more accurately as described in Section 3.1. Based on this, we construct the factor graph and design the MP algorithm for the realization of module B, as described in the following Sections.

3.3 Probability Representation and Factor Graph

In this subsection, we use Bayesian theory to model module B in the AF domain and represent it as a factor graph. A basic assumption is modeling $\mathbf{h}_B^{\text{pri}(p)}$ as an AWGN observation, i.e.,

$$\mathbf{h}_B^{\text{pri}(p)} = \mathbf{h}_a^{(p)} + \mathbf{n}_a^{(p)}, \quad 1 \leq p \leq P, \quad (20)$$

where $\mathbf{n}_a^{(p)} \sim \mathcal{CN}(\mathbf{0}, v_B^{\text{pri}(p)} \mathbf{I})$ is independent from $\mathbf{h}_a^{(p)}$. Similar assumption have been commonly applied in iterative signal recovery methods based on MP, such as [13, 18, 20, 21]. Under this assumption, and based on (12), we can factorize the joint PDF of all unknown random variables conditioned to the observation $\mathbf{Y}_f = [\mathbf{y}_f^{(1)}, \dots, \mathbf{y}_f^{(P)}]$ as

$$p(\mathbf{H}_a, \mathbf{s}, \mathbf{v}_L, \mathbf{v}_S, p_{10}, p_{01} | \mathbf{Y}_f) \propto \prod_{p=1}^P \prod_{n=1}^N f_{B_n^{(p)}}(\mathbf{h}_{B,n}^{\text{pri}(p)}, \mathbf{h}_{a,n}^{(p)}) f_{g_n^{(p)}}(\mathbf{h}_{a,n}^{(p)}, s_n, v_{L,n}^{(p)}, v_S^{(p)}) \quad (21)$$

$$f_{v_{L,n}^{(p)}}(v_{L,n}^{(p)}) \prod_{p=1}^P f_{v_S^{(p)}}(v_S^{(p)}) \prod_{n=2}^N f_{d_n}(s_n, s_{n-1}, p_{10}, p_{01}) f_{d_1}(s_1, p_{10}) f_{p_{01}}(p_{01}) f_{p_{10}}(p_{10}),$$

where $\mathbf{H}_a = [\mathbf{h}_a^{(1)}, \dots, \mathbf{h}_a^{(P)}]$ is the collection of the AF domain channel vectors. The functions of factor nodes are listed in Table 2, while the aforementioned factorization is illustrated in Fig. 4. Based on this factor graph, we will design the MP algorithm in the next Section.

4 Hybrid message passing channel estimation algorithm

In this section, we propose the HMP-TSGM-LVD algorithm. Firstly, we divide all edges in the factor graph shown in Fig. 4 into two categories based on the relationship between factors and variables, then calculate messages using the HMP rule, as described in Section 2. Next, we present the message calculations in five parts, following the message delivery direction. Finally, we summarize the overall HMP-TSGM-LVD algorithm message scheduling.

⁶The extrinsic messages are calculated by dividing two Gaussian PDFs, e.g., $v_A^{\text{ext}(p)-1} = v_A^{\text{post}(p)-1} - v_A^{\text{pri}(p)-1}$, $\mathbf{h}_A^{\text{ext}(p)} = v_A^{\text{ext}(p)}(\mathbf{h}_A^{\text{post}(p)} / v_A^{\text{post}(p)} - \mathbf{h}_A^{\text{pri}(p)} / v_A^{\text{pri}(p)})$.

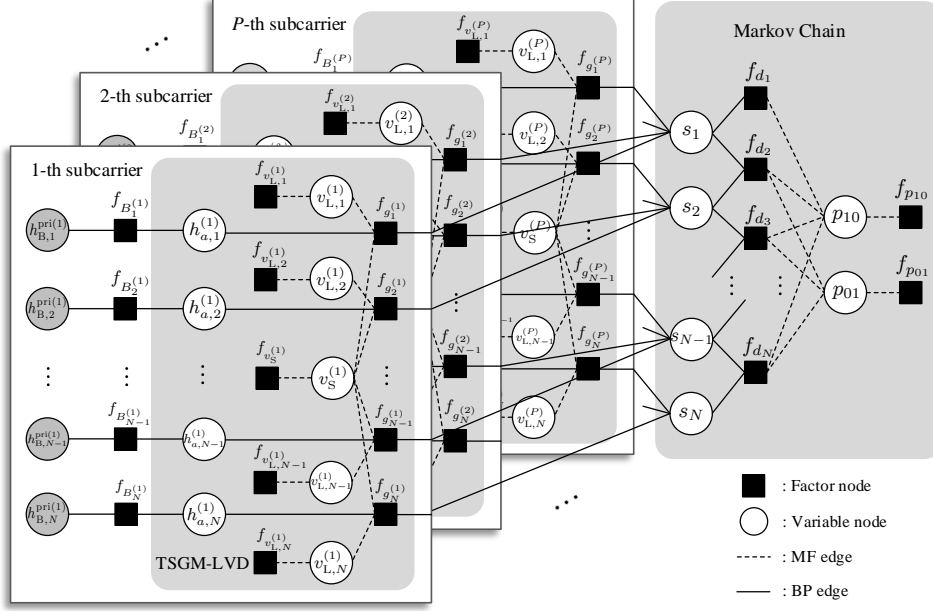


Figure 4: Factor graph representing the probability model of (21). The white circles, black squares and shaded gray circles represent the variable nodes, factor nodes and the observations, respectively. Note that the observations are the extrinsic messages coming from module A.

Table 2: Functions of the factor nodes in Fig. 4.

Factor Node	Factor Function
$f_{B_n}^{(p)}$	$p(h_{a,n}^{(p)} h_{B,n}^{\text{pri}(p)}) = \mathcal{CN}(h_{a,n}^{(p)}; h_{B,n}^{\text{pri}(p)}, v_B^{\text{pri}(p)})$
$f_{g_n}^{(p)}$	$p(h_{a,n}^{(p)} s_n, v_{L,n}^{(p)}, v_S^{(p)}) = \delta(s_n) \mathcal{CN}(h_{a,n}^{(p)}; 0, v_S^{(p)-1}) + \delta(1-s_n) \mathcal{CN}(h_{a,n}^{(p)}; 0, v_{L,n}^{(p)-1})$
$f_{v_{L,n}}^{(p)}$	$p(v_{L,n}^{(p)}) = \text{Ga}(v_{L,n}^{(p)}; \epsilon_n^{(p)}, \eta_n^{(p)})$
$f_{v_S}^{(p)}$	$p(v_S^{(p)}) = \text{Ga}(v_S^{(p)}; \alpha^{(p)}, \beta^{(p)})$
f_{d_n}	$p(s_n, s_{n-1} p_{10}, p_{01}) = [(1-p_{10})^{\delta(s_n)} (p_{10})^{\delta(1-s_n)}]^{\delta(s_{n-1})} [(p_{01})^{\delta(s_n)} (1-p_{01})^{\delta(1-s_n)}]^{\delta(1-s_{n-1})}$
f_{d_1}	$p(s_1 p_{10}) = (p_{10})^{\delta(1-s_1)} (1-p_{10})^{\delta(s_1)}$
$f_{p_{01}}$	$p(p_{01}) = \text{Beta}(p_{01}; c, d)$
$f_{p_{10}}$	$p(p_{10}) = \text{Beta}(p_{10}; e, f)$

4.1 Calculation of Messages

All the factors in Table 2 are collected in the set $\mathcal{A}_{\text{Hybrid}}$; we group the edges as two disjoint subsets \mathcal{E}_{BP} and \mathcal{E}_{MF} , as shown in Fig. 4. We use the solid lines to denote BP edges, dashed lines for MF edges. The message calculations on the BP edges employ (5) and (6), while (7), (8) and (9) are used to calculate the messages on the MF edges. We divide the messages calculation into five parts, according to the direction of the delivered message: right part, downward part, upward part⁷, transition probability hyperparameters update part and left part.

⁷The downward and upward parts are based on the Markov chain formulation, and their complete name should be named Markov chain downward and Markov chain upward parts. For the sake of simplicity, the term Markov chain will be omitted in the following Sections.

4.1.1 Right part messages

since the edge connect with $f_{B_n^{(p)}}$ and $h_{a,n}^{(p)}$ belong to \mathcal{E}_{BP} , the extrinsic message passed from $f_{B_n^{(p)}}$ to $h_{a,n}^{(p)}$ can be expressed as

$$m_{f_{B_n^{(p)}} \rightarrow h_{a,n}^{(p)}}^{\text{BP}}(h_{a,n}^{(p)}) = \mathcal{CN}(h_{a,n}^{(p)}; h_{B,n}^{\text{pri}(p)}, v_B^{\text{pri}(p)}), \quad (22)$$

where $h_{B,n}^{\text{pri}(p)}, v_B^{\text{pri}(p)}$ are based on AWGN observation, as described in (20). Note that $n_{h_{a,n}^{(p)} \rightarrow f_{g_n^{(p)}}}^{\text{BP}}(h_{a,n}^{(p)})$ is the same as $m_{f_{B_n^{(p)}} \rightarrow h_{a,n}^{(p)}}^{\text{BP}}(h_{a,n}^{(p)})$. According to the assumption of Gamma distributed precision terms, the beliefs $b(v_{L,n}^{(p)})$ and $b(v_S^{(p)})$ follow $\text{Ga}(v_{L,n}^{(p)}; \hat{\epsilon}_n^{(p)}, \hat{\eta}_n^{(p)})$ and $\text{Ga}(v_S^{(p)}; \hat{\alpha}^{(p)}, \hat{\beta}^{(p)})$, whose parameters are updated in (56) and (57), respectively. Then, the message $m_{f_{g_n^{(p)}} \rightarrow s_n}^{\text{BP}}(s_n)$ uses the HMP rule (5), resulting in

$$\begin{aligned} m_{f_{g_n^{(p)}} \rightarrow s_n}^{\text{BP}}(s_n) &= \int \exp\left\{ \langle \ln f_{g_n^{(p)}} \rangle_{b(v_S^{(p)})b(v_{L,n}^{(p)})} \right\} n_{h_{a,n}^{(p)} \rightarrow f_{g_n^{(p)}}}(h_{a,n}^{(p)}) dh_{a,n}^{(p)} \\ &= \bar{\pi}_n^{(p)} \delta(1 - s_n) + (1 - \bar{\pi}_n^{(p)}) \delta(s_n), \end{aligned} \quad (23)$$

where

$$\bar{\pi}_n^{(p)} \triangleq \frac{\frac{e^{\psi(\hat{\epsilon}_n^{(p)})}}{\hat{\epsilon}_n^{(p)}} \mathcal{CN}(h_{B,n}^{\text{pri}(p)}; 0, v_B^{\text{pri}(p)} + \frac{\hat{\eta}_n^{(p)}}{\hat{\epsilon}_n^{(p)}})}{\frac{e^{\psi(\hat{\epsilon}_n^{(p)})}}{\hat{\epsilon}_n^{(p)}} \mathcal{CN}(h_{B,n}^{\text{pri}(p)}; 0, v_B^{\text{pri}(p)} + \frac{\hat{\eta}_n^{(p)}}{\hat{\epsilon}_n^{(p)}}) + \frac{e^{\psi(\hat{\alpha}^{(p)})}}{\hat{\alpha}^{(p)}} \mathcal{CN}(h_{B,n}^{\text{pri}(p)}; 0, v_B^{\text{pri}(p)} + \frac{\hat{\beta}^{(p)}}{\hat{\alpha}^{(p)}})}}, \quad (24)$$

and $\psi(x) \triangleq \ln x - \frac{1}{2x}$.

4.1.2 Downward part messages

According to the assumption of beliefs $b(p_{10}) = \text{Beta}(p_{10}; \hat{e}, \hat{f})$ and $b(p_{10}) = \text{Beta}(p_{01}; \hat{c}, \hat{d})$, whose parameters are updated later in (45) and (46), the message from factor node f_{d_1} to variable node s_1 employs HMP rule (5). The message results

$$m_{f_{d_1} \rightarrow s_1}^{\text{BP}}(s_1) = \exp\{ \langle \ln f_{d_1} \rangle_{b(p_{10})} \} = \lambda_1^\downarrow \delta(1 - s_1) + (1 - \lambda_1^\downarrow) \delta(s_1), \quad (25)$$

where

$$\lambda_1^\downarrow \triangleq \frac{\exp\{ \langle \ln p_{10} \rangle \}}{\exp\{ \langle \ln p_{10} \rangle \} + \exp\{ \langle \ln(1 - p_{10}) \rangle \}}, \quad (26)$$

and

$$\langle \ln p_{10} \rangle = \psi(\hat{e}) - \psi(\hat{e} + \hat{f}), \quad \langle \ln(1 - p_{10}) \rangle = \psi(\hat{f}) - \psi(\hat{e} + \hat{f}). \quad (27)$$

Then, the message from variable node s_n to factor nodes $f_{d_{n+1}}$ uses (6), obtaining

$$n_{s_n \rightarrow f_{d_{n+1}}}^{\text{BP}}(s_n) = \lambda_n^\downarrow \delta(1 - s_n) + (1 - \lambda_n^\downarrow) \delta(s_n), \quad 1 \leq n \leq N - 1, \quad (28)$$

where

$$\lambda_n^\downarrow \triangleq \frac{\lambda_n^\downarrow \prod_{p=1}^P \bar{\pi}_n^{(p)}}{\lambda_n^\downarrow \prod_{p=1}^P \bar{\pi}_n^{(p)} + (1 - \lambda_n^\downarrow) \prod_{p=1}^P (1 - \bar{\pi}_n^{(p)})}, \quad (29)$$

Similar to (25), the message $m_{f_{d_n} \rightarrow s_n}^{\text{BP}}(s_n)$ is obtained by the HMP rule (5) as

$$\begin{aligned} m_{f_{d_n} \rightarrow s_n}^{\text{BP}}(s_n) &= \int \exp\{ \langle \ln f_{d_n} \rangle_{b(p_{10})b(p_{01})} \} n_{s_{n-1} \rightarrow f_{d_n}}(s_{n-1}) ds_{n-1} \\ &= \lambda_n^\downarrow \delta(1 - s_n) + (1 - \lambda_n^\downarrow) \delta(s_n), \quad 2 \leq n \leq N - 1, \end{aligned} \quad (30)$$

where

$$\lambda_n^\downarrow \triangleq \frac{\lambda_{n-1}^\downarrow \text{Con1} + (1 - \lambda_{n-1}^\downarrow) \text{Con2}}{\lambda_{n-1}^\downarrow (\text{Con1} + \text{Con4}) + (1 - \lambda_{n-1}^\downarrow) (\text{Con2} + \text{Con3})}, \quad (31)$$

and

$$\begin{aligned} \text{Con1} &= \exp\{ \langle \ln(1 - p_{01}) \rangle \}; \quad \text{Con2} = \exp\{ \langle \ln p_{10} \rangle \}; \\ \text{Con3} &= \exp\{ \langle \ln(1 - p_{10}) \rangle \}; \quad \text{Con4} = \exp\{ \langle \ln p_{01} \rangle \}; \\ \langle \ln p_{01} \rangle &= \psi(\hat{c}) - \psi(\hat{c} + \hat{d}), \quad \langle \ln(1 - p_{01}) \rangle = \psi(\hat{d}) - \psi(\hat{c} + \hat{d}). \end{aligned} \quad (32)$$

4.1.3 Upward part messages

First, we initialize $\lambda_N^\uparrow = 1/2$. The message $n_{s_n \rightarrow f_{d_n}}^{\text{BP}}(s_n)$ from s_n to f_{d_n} results

$$n_{s_n \rightarrow f_{d_n}}^{\text{BP}}(s_n) = \lambda_n^\uparrow \delta(1 - s_n) + (1 - \lambda_n^\uparrow) \delta(s_n), \quad 1 \leq n \leq N, \quad (33)$$

where

$$\lambda_n^\uparrow \triangleq \frac{\lambda_n^\uparrow \prod_{p=1}^P \bar{\pi}_n^{(p)}}{\lambda_n^\uparrow \prod_{p=1}^P \bar{\pi}_n^{(p)} + (1 - \lambda_n^\uparrow) \prod_{p=1}^P (1 - \bar{\pi}_n^{(p)})}. \quad (34)$$

Then, we can compute the message from $f_{d_{n+1}}$ to s_n by the HMP rule (5), as follows

$$m_{f_{d_{n+1}} \rightarrow s_n}^{\text{BP}}(s_n) = \lambda_n^\uparrow \delta(1 - s_n) + (1 - \lambda_n^\uparrow) \delta(s_n), \quad 1 \leq n \leq N - 1, \quad (35)$$

where

$$\lambda_n^\uparrow \triangleq \frac{\lambda_{n+1}^\uparrow \text{Con1} + (1 - \lambda_{n+1}^\uparrow) \text{Con4}}{\lambda_{n+1}^\uparrow (\text{Con1} + \text{Con2}) + (1 - \lambda_{n+1}^\uparrow) (\text{Con3} + \text{Con4})}, \quad (36)$$

where Con1, Con2, Con3, Con4 are defined in (32).

4.1.4 Transition probability hyperparameters update part messages

The belief $b(s_1)$ and the combined belief $b(s_n, s_{n-1}), 2 \leq n \leq N$ are calculated by (8), resulting in

$$b(s_1) = B_{s_1} \delta(1 - s_1) + (1 - B_{s_1}) \delta(s_1), \quad (37)$$

$$b(s_n, s_{n-1}) = \frac{1}{\rho_{n,n-1}} [B_{n,n-1}^{00} \delta(s_n) \delta(s_{n-1}) + B_{n,n-1}^{01} \delta(s_n) \delta(1 - s_{n-1}) + B_{n,n-1}^{10} \delta(1 - s_n) \delta(s_{n-1}) + B_{n,n-1}^{11} \delta(1 - s_n) \delta(1 - s_{n-1})], \quad (38)$$

where the normalized factors are

$$B_{s_1} \triangleq \frac{\lambda_1^\uparrow \lambda_1^\downarrow \prod_{p=1}^P \bar{\pi}_1^{(p)}}{\lambda_1^\uparrow \lambda_1^\downarrow \prod_{p=1}^P \bar{\pi}_1^{(p)} + (1 - \lambda_1^\uparrow) (1 - \lambda_1^\downarrow) \prod_{p=1}^P (1 - \bar{\pi}_1^{(p)})}, \quad (39)$$

$$\begin{aligned} B_{n,n-1}^{00} &= (1 - \lambda_n^\uparrow) (1 - \lambda_{n-1}^\downarrow) \exp\{\langle \ln(1 - p_{10}) \rangle\}, \\ B_{n,n-1}^{01} &= (1 - \lambda_n^\uparrow) \lambda_{n-1}^\downarrow \exp\{\langle \ln p_{01} \rangle\}, \\ B_{n,n-1}^{10} &= \lambda_n^\uparrow (1 - \lambda_{n-1}^\downarrow) \exp\{\langle \ln p_{10} \rangle\}, \\ B_{n,n-1}^{11} &= \lambda_n^\uparrow \lambda_{n-1}^\downarrow \exp\{\langle \ln(1 - p_{01}) \rangle\}, \\ \rho_{n,n-1} &= B_{n,n-1}^{00} + B_{n,n-1}^{01} + B_{n,n-1}^{10} + B_{n,n-1}^{11}. \end{aligned} \quad (40)$$

Then, we can apply HMP rule (7) to calculate the messages from f_{d_1} to p_{10} and f_{d_n} to $p_{10}, p_{01}, 2 \leq n \leq N$ as

$$m_{f_{d_1} \rightarrow p_{10}}^{\text{MF}}(p_{10}) = \exp\{\langle \ln f_{d_1} \rangle_{b(s_1)}\} \propto \text{Beta}(p_{10}; B_{s_1} + 1, 2 - B_{s_1}), \quad (41)$$

$$m_{f_{d_n} \rightarrow p_{10}}^{\text{MF}}(p_{10}) = \exp\{\langle \ln f_{d_n} \rangle_{b(s_n, s_{n-1}) b(p_{01})}\} \propto \text{Beta}\left(p_{10}; \frac{B_{n,n-1}^{10}}{\rho_{n,n-1}} + 1, \frac{B_{n,n-1}^{00}}{\rho_{n,n-1}} + 1\right), \quad (42)$$

$$m_{f_{d_n} \rightarrow p_{01}}^{\text{MF}}(p_{01}) = \exp\{\langle \ln f_{d_n} \rangle_{b(s_n, s_{n-1}) b(p_{10})}\} \propto \text{Beta}\left(p_{01}; \frac{B_{n,n-1}^{01}}{\rho_{n,n-1}} + 1, \frac{B_{n,n-1}^{11}}{\rho_{n,n-1}} + 1\right). \quad (43)$$

Given $m_{f_{p_{10}} \rightarrow p_{10}}^{\text{MF}}(p_{10}) = \text{Beta}(p_{10}; e, f)$ and $m_{f_{p_{01}} \rightarrow p_{01}}^{\text{MF}}(p_{01}) = \text{Beta}(p_{01}; c, d)$, the beliefs $b(p_{10})$ and $b(p_{01})$ of variables p_{10} and p_{01} read

$$b(p_{10}) \propto \text{Beta}(p_{10}; \hat{e}, \hat{f}), \quad b(p_{01}) \propto \text{Beta}(p_{01}; \hat{c}, \hat{d}), \quad (44)$$

whose parameters are updated through

$$\hat{e} = B_{s_1} + e + \sum_{n=2}^N \frac{B_{n,n-1}^{10}}{\rho_{n,n-1}}; \quad \hat{f} = 1 - B_{s_1} + f + \sum_{n=2}^N \frac{B_{n,n-1}^{00}}{\rho_{n,n-1}}, \quad (45)$$

$$\hat{c} = c + \sum_{n=2}^N \frac{B_{n,n-1}^{01}}{\rho_{n,n-1}}; \quad \hat{d} = d + \sum_{n=2}^N \frac{B_{n,n-1}^{11}}{\rho_{n,n-1}}. \quad (46)$$

4.1.5 Left part messages

We update downward and upward messages in *Part 2* and *Part 3* again using the beliefs $b(p_{10})$ and $b(p_{01})$ updated through (45) and (46), to increase the estimation performance. Then, the message going out of the Markov chain $n_{s_n \rightarrow f_{g_n}^{BP}}(s_n)$ from s_n to $f_{g_n}^{(p)}$ is updated by

$$n_{s_n \rightarrow f_{g_n}^{(p)}}^{BP}(s_n) = \bar{\pi}_n^{(p)} \delta(1 - s_n) + (1 - \bar{\pi}_n^{(p)}) \delta(s_n), \quad 1 \leq n \leq N, 1 \leq p \leq P, \quad (47)$$

where

$$\bar{\pi}_n^{(p)} \triangleq \frac{\lambda_n^\uparrow \lambda_n^\downarrow \prod_{p' \neq p}^P \bar{\pi}_n^{(p')}}{\lambda_n^\uparrow \lambda_n^\downarrow \prod_{p' \neq p}^P \bar{\pi}_n^{(p')} + (1 - \lambda_n^\uparrow)(1 - \lambda_n^\downarrow) \prod_{p' \neq p}^P (1 - \bar{\pi}_n^{(p')})}. \quad (48)$$

In order to use HMP rule to update the variances of the TSGM-LVD prior model, we first calculate the combined belief $b(h_{a,n}^{(p)}, s_n)$ using (8) as

$$b(h_{a,n}^{(p)}, s_n) = B_{h_n, s_n}^{(p)} \delta(1 - s_n) \mathcal{CN}(h_{a,n}^{(p)}, \hat{\mu}_{L,n}^{(p)}, \hat{\zeta}_{L,n}^{(p)}) + (1 - B_{h_n, s_n}^{(p)}) \delta(s_n) \mathcal{CN}(h_{a,n}^{(p)}, \hat{\mu}_{S,n}^{(p)}, \hat{\zeta}_{S,n}^{(p)}), \quad (49)$$

where

$$B_{h_n, s_n}^{(p)} \triangleq \frac{\bar{\pi}_n^{(p)} \bar{\pi}_n^{(p)}}{\bar{\pi}_n^{(p)} \bar{\pi}_n^{(p)} + (1 - \bar{\pi}_n^{(p)})(1 - \bar{\pi}_n^{(p)})}, \quad (50)$$

$$\hat{\zeta}_{L,n}^{(p)} = (v_B^{\text{pri}(p)-1} + \hat{\epsilon}_n^{(p)} / \hat{\eta}_n^{(p)})^{-1}, \quad \hat{\mu}_{L,n}^{(p)} = \hat{\zeta}_{L,n}^{(p)} h_{B,n}^{\text{pri}(p)} / v_B^{\text{pri}(p)}; \quad (51)$$

$$\hat{\zeta}_{S,n}^{(p)} = (v_B^{\text{pri}(p)-1} + \hat{\alpha}^{(p)} / \hat{\beta}^{(p)})^{-1}, \quad \hat{\mu}_{S,n}^{(p)} = \hat{\zeta}_{S,n}^{(p)} h_{B,n}^{\text{pri}(p)} / v_B^{\text{pri}(p)}. \quad (52)$$

Then, the messages from $f_{g_n}^{(p)}$ to variable nodes $v_{L,n}^{(p)}$ and $v_{S,n}^{(p)}$ can be computed with the HMP rule (7) as

$$m_{f_{g_n}^{(p)} \rightarrow v_{L,n}^{(p)}}^{\text{MF}}(v_{L,n}^{(p)}) = \exp\left\{ \langle \ln f_{g_n}^{(p)} \rangle_{b(h_{a,n}^{(p)}, s_n) b(v_{S,n}^{(p)})} \right\} \\ \propto \text{Ga}(v_{L,n}^{(p)}; 1 + B_{h_n, s_n}, B_{h_n, s_n} (|\hat{\mu}_{L,n}^{(p)}|^2 + \hat{\zeta}_{L,n}^{(p)})), \quad (53)$$

$$m_{f_{g_n}^{(p)} \rightarrow v_{S,n}^{(p)}}^{\text{MF}}(v_{S,n}^{(p)}) = \exp\left\{ \langle \ln f_{g_n}^{(p)} \rangle_{b(h_{a,n}^{(p)}, s_n) b(v_{L,n}^{(p)})} \right\} \\ \propto \text{Ga}(v_{S,n}^{(p)}; 2 - B_{h_n, s_n}, (1 - B_{h_n, s_n}) (|\hat{\mu}_{S,n}^{(p)}|^2 + \hat{\zeta}_{S,n}^{(p)})). \quad (54)$$

Given the prior distributions of $v_{L,n}^{(p)}$ and $v_{S,n}^{(p)}$, i.e., $m_{f_{v_{L,n}^{(p)}} \rightarrow v_{L,n}^{(p)}}^{\text{MF}}(v_{L,n}^{(p)}) = \text{Ga}(v_{L,n}^{(p)}; \epsilon_n^{(p)}, \eta_n^{(p)})$ and $m_{f_{v_{S,n}^{(p)}} \rightarrow v_{S,n}^{(p)}}^{\text{MF}}(v_{S,n}^{(p)}) = \text{Ga}(v_{S,n}^{(p)}; \alpha^{(p)}, \beta^{(p)})$, we can update the beliefs $b(v_{L,n}^{(p)})$ and $b(v_{S,n}^{(p)})$ as

$$b(v_{L,n}^{(p)}) = \text{Ga}(v_{L,n}^{(p)}; \hat{\epsilon}_n^{(p)}, \hat{\eta}_n^{(p)}), \quad b(v_{S,n}^{(p)}) = \text{Ga}(v_{S,n}^{(p)}; \hat{\alpha}^{(p)}, \hat{\beta}^{(p)}), \quad (55)$$

whose parameters are updated through

$$\hat{\epsilon}_n^{(p)} = \epsilon_n^{(p)} + B_{h_n, s_n}, \quad \hat{\eta}_n^{(p)} = \eta_n^{(p)} + B_{h_n, s_n} (|\hat{\mu}_{L,n}^{(p)}|^2 + \hat{\zeta}_{L,n}^{(p)}); \quad (56)$$

$$\hat{\alpha}^{(p)} = \alpha^{(p)} + \sum_{n=1}^N (1 - B_{h_n, s_n}), \quad \hat{\beta}^{(p)} = \beta^{(p)} + \sum_{n=1}^N (1 - B_{h_n, s_n}) (|\hat{\mu}_{S,n}^{(p)}|^2 + \hat{\zeta}_{S,n}^{(p)}). \quad (57)$$

With the parameters updated in (56) and (57), we can compute the messages $m_{f_{g_n}^{(p)} \rightarrow h_{a,n}^{(p)}}^{\text{BP}}(h_{a,n}^{(p)})$ from $f_{g_n}^{(p)}$ to $h_{a,n}^{(p)}$ by HMP rule (5) as

$$m_{f_{g_n}^{(p)} \rightarrow h_{a,n}^{(p)}}^{\text{BP}}(h_{a,n}^{(p)}) = \int \exp\left\{ \langle \ln f_{g_n}^{(p)} \rangle_{b(v_{L,n}^{(p)}) b(v_{S,n}^{(p)})} \right\} n_{s_n \rightarrow f_{g_n}^{(p)}}(s_n) ds_n \\ = \bar{\pi}_n^{(p)} \frac{e^{\psi(\hat{\epsilon}_n^{(p)})}}{\hat{\epsilon}_n^{(p)}} \mathcal{CN}\left(h_{a,n}^{(p)}; 0, \frac{\hat{\eta}_n^{(p)}}{\hat{\epsilon}_n^{(p)}}\right) + (1 - \bar{\pi}_n^{(p)}) \frac{e^{\psi(\hat{\alpha}^{(p)})}}{\hat{\alpha}^{(p)}} \mathcal{CN}\left(h_{a,n}^{(p)}; 0, \frac{\hat{\beta}^{(p)}}{\hat{\alpha}^{(p)}}\right), \quad (58)$$

Therefore, we can get the belief $b(h_{a,n}^{(p)})$ of $h_{a,n}^{(p)}$ as

$$\begin{aligned} b(h_{a,n}^{(p)}) &= m_{f_{B_n^{(p)}} \rightarrow h_{a,n}^{(p)}}^{\text{BP}}(h_{a,n}^{(p)}) m_{f_{g_n^{(p)}} \rightarrow h_{a,n}^{(p)}}^{\text{BP}}(h_{a,n}^{(p)}) \\ &= B_{h_n}^{(p)} \mathcal{CN}(h_{a,n}^{(p)}, \hat{\mu}_{L,n}^{(p)}, \hat{\varsigma}_{L,n}^{(p)}) + (1 - B_{h_n}^{(p)}) \mathcal{CN}(h_{a,n}^{(p)}, \hat{\mu}_{S,n}^{(p)}, \hat{\varsigma}_S^{(p)}), \end{aligned} \quad (59)$$

where the parameters $B_{h_n}^{(p)}, \{\hat{\varsigma}_{L,n}^{(p)}, \hat{\mu}_{L,n}^{(p)}\}, \{\hat{\varsigma}_S^{(p)}, \hat{\mu}_{S,n}^{(p)}\}$ are calculated again through (50), (51) and (52), respectively. However, here, the parameters $\hat{\epsilon}_n^{(p)}, \hat{\eta}_n^{(p)}, \hat{\alpha}^{(p)}, \hat{\beta}^{(p)}$ used in (50), (51) and (52) are updated by (56) and (57).

Finally, the output of module B is the mean and variance of the belief $b(h_{a,n}^{(p)})$ as

$$h_{B,n}^{\text{post}(p)} = \mathbb{E} [h_{a,n}^{(p)}] = B_{h_n}^{(p)} \hat{\mu}_{L,n}^{(p)} + (1 - B_{h_n}^{(p)}) \hat{\mu}_{S,n}^{(p)}, \quad (60)$$

$$\begin{aligned} v_B^{\text{post}(p)} &= \frac{1}{N} \sum_{n=1}^N \text{Var} (h_{a,n}^{(p)}) = \frac{1}{N} \sum_{n=1}^N \left\{ B_{h_n}^{(p)} (|\hat{\mu}_{L,n}^{(p)}|^2 + \hat{\varsigma}_{L,n}^{(p)}) + \right. \\ &\quad \left. (1 - B_{h_n}^{(p)}) (|\hat{\mu}_{S,n}^{(p)}|^2 + \hat{\varsigma}_S^{(p)}) - |h_{B,n}^{\text{post}(p)}|^2 \right\}. \end{aligned} \quad (61)$$

4.2 Scheduling of the Messages

The factors in Fig. 4 are very densely connected and thus there are a multitude of different options for message scheduling. We summarize our schedule and the corresponding message computations in **Algorithm 1**. As shown in **Algorithm 1**, some variables are initialized before the iterative process. The detailed initialization values of the parameters are given in the next Section. The *Part 1* messages are first calculated in parallel for each subcarrier based on the extrinsic messages from module A. When the messages over all the subcarriers reach the Markov chain, the *Part 2* and *Part 3* messages are then updated in sequence, respectively. After that, we can update the hyperparameters p_{10} and p_{01} in the *Part 4*. Finally, we can get more accurate *Part 5* messages outgoing the Markov chain by updating the *Part 2* and *Part 3* messages again based on the updated hyperparameters p_{10} and p_{01} from the *Part 4*.

5 Simulation Results

In this section, we first develop the SE to accurately predict the performance of the proposed HMP-TSGM-LVD algorithm. Then, we compare the performance of various algorithms using the channel generated in Section II-A. Previous works [19–21] have demonstrated that STCS-FS performs better than Turbo-CS [18], OMP [35], DSAMP [11], EM-BG-AMP [36], AMP-NNSPL-FD [37]. Hence, as a benchmark, we employ the STCS-FS algorithm [19, 21] which applies the BP-EM to calculate the messages and update the parameters. In order to provide a thorough comparison, we combine the STCS-FS algorithm with BG and TSGM prior probability models. The specific algorithms are labeled as follows: “STCS-FS-BG” and “STCS-FS-TSGM” stand for STCS-FS algorithm with BG [19, 21] and TSGM prior models [15], respectively; “HMP-BG”, “HMP-TSGM” and “HMP-TSGM-LVD” denote the HMP algorithm with BG, TSGM and TSGM-LVD prior models, respectively. It is worth noting that “HMP-TSGM-LVD” denotes the proposed Algorithm 1 when using the proposed probability model, while the HMP-TSGM uses the same Algorithm 1 but it differs in the channel prior model. In particular, TSGM assume that the variances of the non-zero elements are the same. For this scheme, (56) can be replaced by

$$\hat{\epsilon}^{(p)} = \epsilon^{(p)} + \sum_{n=1}^N B_{h_n, s_n}, \quad \hat{\eta}^{(p)} = \eta^{(p)} + \sum_{n=1}^N B_{h_n, s_n} (|\hat{\mu}_{L,n}^{(p)}|^2 + \hat{\varsigma}_{L,n}^{(p)})$$

and the rows 12-16 of Algorithm 1 changes accordingly.

5.1 Parameter Settings

We consider the massive MIMO-OFDM system in which the BS is equipped with $N = 256$ antennas serving a single antenna user. The BS applies $P = 32$ pilot subcarriers to transmit $M = 103 \approx 0.4N$ training sequences continuously. We generate different pilot matrices $\mathbf{A}^{(p)}$ for different subcarriers by PDFT-RP [19]. The detailed SCM parameters listed in Table 3 are used for all the simulations, if not specified. The parameters $\{\epsilon_n^{(p)} = 1, \eta_n^{(p)} = 1, \forall n, p\}$,

Algorithm 1: HMP-TSGM-LVD algorithm

Input: Module A extrinsic messages $\mathbf{h}_B^{\text{pri}(p)}$, $v_B^{\text{pri}(p)}$, $\forall p$, Maximum iterations T .

Output: Module B channel estimation matrix $\mathbf{h}_B^{\text{post}(p)}$, $\forall p$.

Initialize: Prior distribution parameters : $\epsilon_n^{(p)}$, $\eta_n^{(p)}$, $\alpha^{(p)}$, $\beta^{(p)}$, $\forall n, \forall p$; e, f, c, d .

 Belief parameters : $\hat{\epsilon}_n^{(p)}$, $\hat{\eta}_n^{(p)}$, $\hat{\alpha}^{(p)}$, $\hat{\beta}^{(p)}$, $\forall n, \forall p$; $\hat{e}, \hat{f}, \hat{c}, \hat{d}$, and $\lambda_N^\dagger = 1/2$.

```

1 while convergence == FALSE or the iteration number less than T do
    // Part 1 - Right part messages
2    $\forall p, \forall n$ : update  $\bar{\pi}_n^{(p)}$  by (24)
    // Part 2 - Downward messages
3   update  $\lambda_1^\dagger$  and  $\lambda_1^\ddagger$  by (26) and (29)
4    $\forall n \in [2 : N]$ : update  $\lambda_n^\dagger$  and  $\lambda_n^\ddagger$  by (31) and (29)
    // Part 3 - Upward messages
5    $\forall n \in [N - 1 : 1]$ : update  $\lambda_n^\ddagger$  and  $\lambda_n^\dagger$  by (34) and (36)
    // Part 4 - Transition probability parameters update messages
6   update  $B_{s_1}$  by (39)
7    $\forall n \in [2 : N]$ : update  $B_{n,n-1}^{00}$ ,  $B_{n,n-1}^{01}$ ,  $B_{n,n-1}^{10}$ ,  $B_{n,n-1}^{11}$ ,  $\rho_{n,n-1}$  by (40)
8   update  $\hat{e}, \hat{f}$  and  $\hat{c}, \hat{d}$  by (45) and (46)
9   perform step 2-4 again
    // Part 5 - Left part messages
10   $\forall p, \forall n$ : update  $\bar{\pi}_n^{(p)}$  by (48)
11   $\forall p, \forall n$ : update  $B_{h_n, s_n}^{(p)}$  by (50)
12   $\forall p, \forall n$ : update  $\hat{\zeta}_{L,n}^{(p)}$ ,  $\hat{\mu}_{L,n}^{(p)}$  and  $\hat{\zeta}_S^{(p)}$ ,  $\hat{\mu}_{S,n}^{(p)}$  by (51) and (52)
13  update  $\hat{\epsilon}_n^{(p)}$ ,  $\hat{\eta}_n^{(p)}$  and  $\hat{\alpha}^{(p)}$ ,  $\hat{\beta}^{(p)}$  by (56) and (57)
14   $\forall p, \forall n$ : update  $B_{h_n}^{(p)}$  by (50)
15   $\forall p, \forall n$ : update  $\hat{\zeta}_{L,n}^{(p)}$ ,  $\hat{\mu}_{L,n}^{(p)}$  and  $\hat{\zeta}_S^{(p)}$ ,  $\hat{\mu}_{S,n}^{(p)}$  by (51) and (52) again
16   $\forall p, \forall n$ : update  $h_{B,n}^{\text{post}(p)}$ ,  $v_B^{\text{post}(p)}$  by (60) and (61)
    
```

Table 3: Parameter settings for the SCM.

Parameter name	Value	Parameter name	Value
NumBsElements N	256	Subcarriers number K	512
NumMsElements	1	Pilot subcarriers P	32
BandWidth	15MHz	Subcarriers spacing	15KHz
CenterFrequency	2GHz	NumPaths	6
Scenarios	Urban macro, Suburban macro		

$\{\alpha^{(p)} = 1, \beta^{(p)} = 0.01, \forall p\}$, $\{e = 1, f = 1\}$ and $\{c = 1, d = 1\}$ ⁸ of the hyperparameters $v_{L,n}^{(p)}$, $v_S^{(p)}$, p_{10} and p_{01} are empirically set, respectively. For the parameters setting of $v_{L,n}^{(p)}$, $v_S^{(p)}$, we can select a threshold value ρ of the channel data modulus squared $|h_{a,n}^{(p)}|^2$ to intercept the non-zero ($|h_{a,n}^{(p)}|^2 > \rho$) and near-zero ($|h_{a,n}^{(p)}|^2 \leq \rho$) elements positions. Then, we calculate the average power of the channel non-zero and near-zero elements separately as the prior characteristics of the channel probability model variance based on $S = 1000$ channel realizations. Here, we have heuristically set $\rho = 0.05$ and obtained the variance of the large and small Gaussians as $v_{L,n}^{(p)} = 1$ and $v_S^{(p)} = 0.01$. According to [39], the shape parameter of the Gamma distribution is usually set to $\epsilon_n^{(p)} = \alpha^{(p)} = 1$. Further, based on the expectation of the Gamma distribution $v_{L,n}^{(p)} = \eta_n^{(p)} / \epsilon_n^{(p)}$ and $v_S^{(p)} = \beta^{(p)} / \alpha^{(p)}$, we set the scale parameters to $\eta_n^{(p)} = 1, \beta^{(p)} = 0.01$ respectively. At the first iteration of the algorithm, the parameters of the beliefs with $v_{L,n}^{(p)}$, $v_S^{(p)}$, p_{10} and p_{01} are also empirically initialized as the value of the prior parameter values, i.e., $\{\hat{\epsilon}_n^{(p)} = \epsilon_n^{(p)}, \hat{\eta}_n^{(p)} = \eta_n^{(p)}, \forall n, \forall p; \hat{\alpha}^{(p)} = \alpha^{(p)}, \hat{\beta}^{(p)} = \beta^{(p)}, \forall p; \hat{e} = e, \hat{f} = f, \hat{c} = c, \hat{d} = d\}$. The reason is that the

⁸According to [38, chapter 6.2], we set the parameters as $e = f = c = d = 1$ and the hyperparameters p_{10}, p_{01} are uniform distributed since we do not know the prior information about the Markov chain transition probabilities.

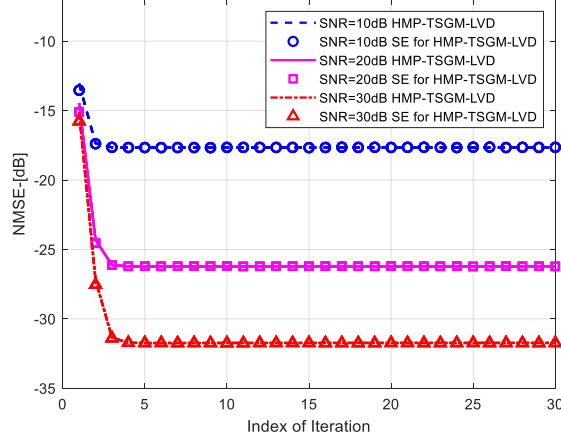


Figure 5: Comparison of SE and simulation results for HMP-TSGM-LVD under different SNR = 10dB, 20dB and 30dB. Both experiments use parameters $N = 512$, $M = 0.8N \approx 400$, and the results are averaged over 100 realizations.

algorithm starts with an initial value for the belief parameters, and then the algorithm will update the belief parameters during each iteration. In addition, it is a reasonable assumption to use the prior values for the initial setting when we do not know the belief parameters.

All the curves are calculated by averaging 100 Monte Carlo simulations. Each simulation employs a new realization of the pilot matrix $\mathbf{A}^{(p)}$, $\forall p$, the channel matrix $\mathbf{h}_a^{(p)}$, $\forall p$ and the AWGN matrix $\boldsymbol{\omega}_f^{(p)}$, $\forall p$. We use the $\text{NMSE} = \|\hat{\mathbf{H}}_a - \mathbf{H}_a\|_2^2 / \|\mathbf{H}_a\|_2^2$ as a performance metric.

5.2 State Evolution

The performance of HMP-TSGM-LVD can be characterized by simple scalar recursions called SE [13, 18, 21, 40]. We use the variance of the extrinsic messages $v_A^{\text{pri}(p)}$ and $v_B^{\text{pri}(p)}$ to measure the reliability of the channel estimator $\mathbf{h}_A^{\text{pri}(p)}$ and $\mathbf{h}_B^{\text{pri}(p)}$, respectively. We define

$$v^{(p)} \triangleq v_A^{\text{pri}(p)} \quad \text{and} \quad \eta^{(p)} \triangleq \frac{1}{v_B^{\text{pri}(p)}}. \quad (62)$$

Moreover, we define $\text{mmse}(\eta^{(p)})$ as the minimum mean squared error (MMSE) of the sparse signal estimation given an AWGN observation, i.e.,

$$\text{mmse}(\eta^{(p)}) = \mathbb{E} \left[\left| h_{a,n}^{(p)} - \mathbb{E} \left[h_{a,n}^{(p)} | h_{a,n}^{(p)} + \xi \right] \right|^2 \right], \quad (63)$$

where $h_{a,n}^{(p)}$ is a sparse signal modeled as (20) and $\xi \sim \mathcal{CN}(0, \eta^{(p)-1})$. Compared with (61), we have

$$v_B^{\text{post}(p)} = \frac{1}{N} \sum_{n=1}^N \text{Var} \left(h_{a,n}^{(p)} | h_{B,n}^{\text{pri}(p)} \right) \longrightarrow \text{mmse}(\eta^{(p)}). \quad (64)$$

Therefore, the SE of the proposed HMP-TSGM-LVD algorithm is characterized by

$$\eta_{t+1}^{(p)} = \varphi(v_t^{(p)}) = \frac{1}{\frac{N}{M} \cdot (v_t^{(p)} + \sigma^2) - v_t^{(p)}}, \quad (65a)$$

$$\frac{1}{v_{t+1}^{(p)}} = \phi(\eta_{t+1}^{(p)}) = \frac{1}{\text{mmse}(\eta_{t+1}^{(p)})} - \eta_{t+1}^{(p)}, \quad (65b)$$

where the subscript t and $t+1$ indicate the iteration indices, and the superscript (p) indicates the pilot subcarrier index. For the detailed derivation of the state evolution in (65) please refers to [18].

Fig. 5 illustrates the NMSE performances of the HMP-TSGM-LVD algorithm proposed in this article, together with the predictions given by the SE (65). We find that HMP-TSGM-LVD convergence can be accurately predicted by the SE, which indicates the effectiveness of the proposed algorithm.

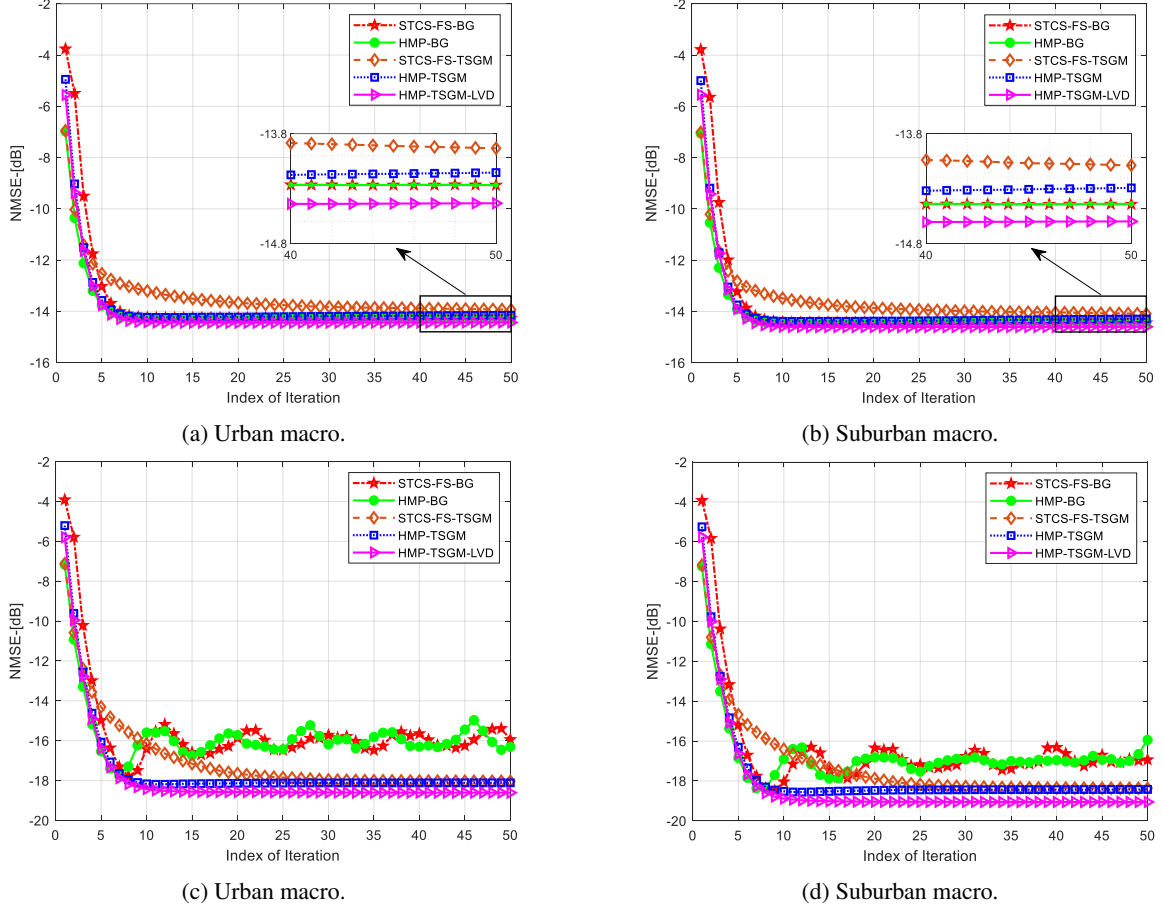


Figure 6: NMSE performance versus iteration index, where the parameter $M = 103$ is used for all subfigures. Subfigure (a), (b) expresses the experimental results for SNR = 15dB in two scenarios, while subfigure (c), (d) are under SNR = 30dB in two scenarios.

5.3 Computational Complexity

Our proposed HMP-TSGM-LVD algorithm has no matrix inverse operation and the complexity is mainly concentrated on matrix multiplication operations. The sensing matrix is chosen as a partial DFT matrix, which means the matrix multiplication can be substituted by FFT. In this way, the complexity of initializing the sensing matrix $\mathbf{A}^{(p)}$, $1 \leq p \leq P$ is $\mathcal{O}(NP \log N)$. The complexity of each iteration attributes to the multiplications computing in line 2, 10-12, 14-16, of which the complexity is approximately $\mathcal{O}(NP)$. Therefore, the overall complexity is $\mathcal{O}(NP \log N + NP)$. This per-iteration complexity is the same as STCS-FS [19, 21], but we will further show that HMP-TSGM-LVD algorithm can achieve better estimation performance than STCS-FS.

5.4 Performance Comparisons

We compare the convergence curves of the NMSE as a function of the number of iterations in Fig. 6. We perform two sets of experiments with signal-to-noise ratio (SNR) = 15dB and SNR = 30dB in the two SCM scenarios: urban macro, and suburban macro. These two scenarios are classified according to the location of the base station and the users [31]. As shown in Figs. 6 (a) and (b), we observe that the performance of the ‘‘HMP-TSGM’’, ‘‘HMP-TSGM-LVD’’ and ‘‘STCS-FS-BG’’ is consistent when SNR = 15dB. However, Figs. 6 (c) and (d) show that ‘‘HMP-TSGM-LVD’’ achieves better performance than other algorithms based on various prior models. This demonstrates that the TSGM-LVD model is able to capture the massive MIMO-OFDM channel characteristics more accurately than the BG or TSGM. In addition, with the same BG or TSGM prior models, HMP based algorithms converge faster than STCS-FS based algorithms while achieving the same performance. It is worth noting that ‘‘HMP-BG’’ and ‘‘STCS-FS-BG’’ exhibit the ‘‘oscillation’’ phenomenon as shown in Figs. 6 (c), (d). The reason for this phenomenon is that, when the

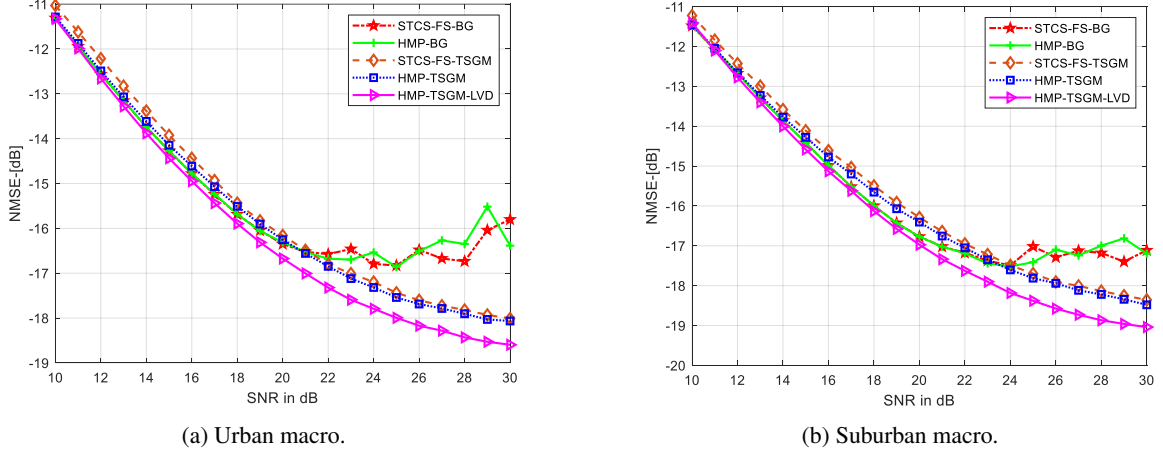


Figure 7: NMSE performance with different SNRs. The system parameters are same in the subfigures with $N = 256$, $M = 103$, $P = 32$.

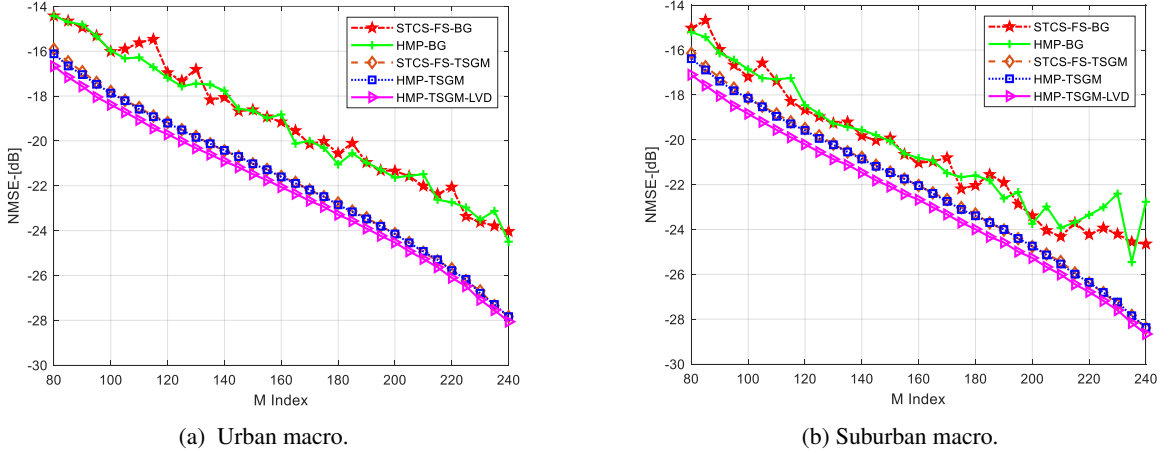


Figure 8: NMSE performance versus the number of pilots $M \in [80 : 240]$. The system parameter is same in all the subfigures: SNR = 30 dB.

SNR is greater than 20 dB, the noise power is less than the power of the near-zero element of the channel. In this case, the channel near-zero elements can be regarded as the main influencing factor for CE, i.e., the BG prior model can not accurately characterize the near-zero elements of the channel.

We compare the average NMSE performance as a function of the SNR in Fig. 7. We can observe that in Figs. 7 (a) and (b), the proposed ‘‘HMP-TSGM-LVD’’ considerably outperforms the other algorithms within high SNR regime, i.e., $\text{SNR} \in [15 : 30]$ dB, while achieves the same performance for $\text{SNR} \in [5 : 15]$ dB. Therefore, the proposed TSGM-LVD prior model is proved to be more suitable to represent the massive MIMO-OFDM channel with different channel conditions.

Finally, Fig. 8 compares the average NMSE performance with a wide range of pilot numbers. Figs. 8 (a) and (b) both demonstrate that ‘‘HMP-TSGM-LVD’’ performs better than any other algorithms regardless of the number of pilots employed. We remark that, under the same experimental conditions, TSGM-LVD model requires fewer pilots to achieve the same performance compared with the BG model. Nevertheless, the performance of HMP-TSGM is consistent with STCS-FS-TSGM, but the former converges faster than the latter proving the effectiveness of our approach.

6 Conclusion

In this article, we investigate the structured Turbo framework channel estimation problem in a massive MIMO-OFDM system. To exploit the sparsity structure of the channel in the AF domain, we proposed the TSGM-LVD probability

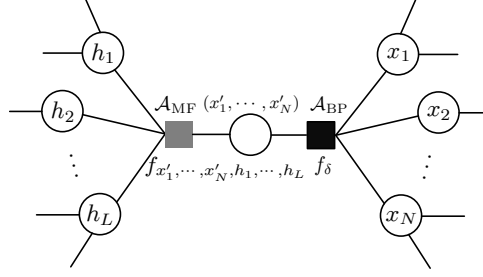


Figure 9: Stretched factor graph.

model. To solve the channel estimation problem in a practical communication system, we proposed a new method to derive the HMP rule, which is able to solve the joint product summation operations at the same factor node. By mixing the prior model and the HMP rule, we designed the HMP-TSGM-LVD channel estimation algorithm. In the simulations, we tested the approach in different SCM scenarios. It was demonstrated that the TSGM-LVD prior model fit the massive MIMO-OFDM channel characteristics better than other models in the literature. Moreover, we showed that the proposed algorithm converges faster and achieves better NMSE performance under a wide range of simulation settings, while having the same complexity as other state-of-the-art algorithms.

A Derivation of Hybrid Message Passing Rule

We consider the partial probability relationship as shown in Fig. 1. Our target is to compute the messages $m_{f_a \rightarrow x_i}(x_i)$, $i \in [1, N]$ and $m_{f_a \rightarrow h_l}(h_l)$, $l \in [1, L]$. We can apply the combined BP-MF rule [14] using the factor graph stretching approach [16] to complete messages calculation. We modify the factor graph in Fig. 1 by adding hard constraint factors $f_\delta \triangleq \delta(x'_1 - x_1) \cdots \delta(x'_N - x_N)$ with a new combined variable (x'_1, \cdots, x'_N) . The new factor graph, shown in Fig. 9, looks like a stretched version of the graph in Fig. 1. In the new graph, we first group the factor nodes into two sets: $\mathcal{A}_{BP} = \{f_\delta\}$ and $\mathcal{A}_{MF} = \{f_{new}\}$ ⁹. For factor nodes in the BP part, we calculate the messages to neighboring variable nodes using (2), and send extrinsic messages. For factor nodes in the MF part, messages to neighboring variable nodes are computed by (3), and beliefs are passed. The messages calculation procedure is presented in the following. The message from factor node f_δ to variable node (x'_1, \cdots, x'_N) use (2) as

$$\begin{aligned} m_{f_\delta \rightarrow x'_1, \dots, x'_N}(x'_1, \dots, x'_N) &= \int \delta(x'_1 - x_1) \cdots \delta(x'_N - x_N) n_{x_1 \rightarrow f_\delta}(x_1) \cdots n_{x_N \rightarrow f_\delta}(x_N) dx_1 \cdots dx_N \\ &= n_{x_1 \rightarrow f_\delta}(x'_1) \cdots n_{x_N \rightarrow f_\delta}(x'_N). \end{aligned} \quad (66)$$

Then, message $m_{f_{new} \rightarrow h_l}(h_l)$ from f_{new} to h_l is obtained by (3),

$$m_{f_{new} \rightarrow h_l}(h_l) = \exp \left\{ \langle \ln f_{new} \rangle_{b(x'_1, \dots, x'_N) \prod_{j \in \mathcal{I}_{MF} \setminus l} b(h_j)} \right\}, \forall l \in \mathcal{I}_{MF}, \quad (67)$$

where the combined belief of (x'_1, \cdots, x'_N) reads

$$b(x'_1, \cdots, x'_N) = m_{f_{new} \rightarrow x'_1, \dots, x'_N}(x'_1, \cdots, x'_N) n_{x_1 \rightarrow f_\delta}(x'_1) \cdots n_{x_N \rightarrow f_\delta}(x'_N). \quad (68)$$

The message $m_{f_{new} \rightarrow x'_1, \dots, x'_N}(x'_1, \cdots, x'_N)$ in (68) is computed with (3), obtaining

$$m_{f_{new} \rightarrow x'_1, \dots, x'_N}(x'_1, \cdots, x'_N) = \exp \left\{ \langle \ln f_{new} \rangle_{\prod_{l \in \mathcal{I}_{MF}} b(h_l)} \right\}, \quad (69)$$

where the beliefs $b(h_l)$, $l \in [1, L]$ are updated by MF rule. Meanwhile, $n_{x'_1, \dots, x'_N \rightarrow f_\delta}(x'_1, \cdots, x'_N)$ is same as (69), i.e.,

$$n_{x'_1, \dots, x'_N \rightarrow f_\delta}(x'_1, \cdots, x'_N) = m_{f_{new} \rightarrow x'_1, \dots, x'_N}(x'_1, \cdots, x'_N). \quad (70)$$

Finally, with the message (70), we can calculate the message $m_{f_\delta \rightarrow x_i}(x_i)$ by BP rule as

$$m_{f_\delta \rightarrow x_i}(x_i) = \int \exp \left\{ \langle \ln f_{new} \rangle_{\prod_{l \in \mathcal{I}_{MF}} b(h_l)} \right\} \prod_{j \in \mathcal{I}_{BP} \setminus i} n_{x_j \rightarrow f_\delta}(x_j) dx_j. \quad (71)$$

We refer to (67), (68) and (71) are HMP rule, which is well-suited to mixed linear and non-linear scenarios, e.g., the channel probability model shown in (14) in Section 3.1.

⁹For simplicity of writing, we define $f_{new} \triangleq f_{x'_1, \dots, x'_N, h_1, \dots, h_L}$.

Acknowledgement

The authors thank Prof. Petar Popovski from Aalborg University, Denmark, for the insightful discussions and suggestions that greatly assisted this work.

References

- [1] L. Lu, G. Y. Li, A. L. Swindlehurst *et al.*, “An overview of massive MIMO: benefits and challenges,” *IEEE J. Sel. Topics Signal Process.*, vol. 8, no. 5, pp. 742–758, May 2014.
- [2] C.-X. Wang, F. Haider, X. Gao *et al.*, “Cellular architecture and key technologies for 5G wireless communication networks,” *IEEE Commun. Mag.*, vol. 52, no. 2, pp. 122–130, Nov. 2014.
- [3] Y. Zhong, J. Wang, S. Wu *et al.*, “Multilocation human activity recognition via MIMO-OFDM based wireless networks: an IoT-inspired device-free sensing approach,” *IEEE Internet Things J.*, vol. 8, no. 20, pp. 15 148–15 159, Oct. 2021.
- [4] J. Choi, D. J. Love, and P. Bidigare, “Downlink training techniques for FDD massive MIMO systems: open-loop and closed-loop training with memory,” *IEEE J. Sel. Topics Signal Process.*, vol. 8, no. 5, pp. 802–814, May 2014.
- [5] D. Angelosante, E. Biglieri, and M. Lops, “Sequential estimation of multipath MIMO-OFDM channels,” *IEEE Trans. Signal Process.*, vol. 57, no. 8, pp. 3167–3181, Aug. 2009.
- [6] D. Tse and P. Viswanath, *Fundamentals of Wireless Communication*. Cambridge, U.K.: Cambridge, Univ. Press, 2005.
- [7] A. Liu, V. K. N. Lau, and W. Dai, “Exploiting burst-sparsity in massive MIMO with partial channel support information,” *IEEE Trans. Wireless Commun.*, vol. 15, no. 11, pp. 7820–7830, Nov. 2016.
- [8] X. Rao and V. K. Lau, “Compressive sensing with prior support quality information and application to massive MIMO channel estimation with temporal correlation,” *IEEE Trans. Signal Process.*, vol. 63, no. 18, pp. 4914–4924, Sep. 2015.
- [9] Y. Han, J. Lee, and D. J. Love, “Compressed sensing-aided downlink channel training for FDD massive MIMO systems,” *IEEE Trans. Commun.*, vol. 65, no. 7, pp. 2852–2862, Jul. 2017.
- [10] Z. Gao, L. Dai, Z. Wang *et al.*, “Spatially common sparsity based adaptive channel estimation and feedback for FDD massive MIMO,” *IEEE Trans. Signal Process.*, vol. 63, no. 23, pp. 6169–6183, Dec. 2015.
- [11] Z. Gao, L. Dai, W. Dai *et al.*, “Structured compressive sensing-based spatio-temporal joint channel estimation for FDD massive MIMO,” *IEEE Trans. Commun.*, vol. 64, no. 2, pp. 601–617, Feb. 2016.
- [12] F. Kschischang, B. Frey, and H.-A. Loeliger, “Factor graphs and the sum-product algorithm,” *IEEE Trans. Inf. Theory*, vol. 47, no. 2, pp. 498–519, Feb. 2001.
- [13] D. L. Donoho, A. Maleki, and A. Montanari, “Message-passing algorithms for compressed sensing,” *Proc. Nat. Acad. Sci. USA*, vol. 106, no. 45, pp. 18 914–18 919, Nov. 2009.
- [14] E. Riegler, G. E. Kirkelund, C. N. Manchon *et al.*, “Merging belief propagation and the mean field approximation: a free energy approach,” *IEEE Trans. Inf. Theory*, vol. 59, no. 1, pp. 588–602, Jan. 2013.
- [15] P. Schniter, “A message-passing receiver for BICM-OFDM over unknown clustered-sparse channels,” *IEEE J. Sel. Topics Signal Process.*, vol. 5, no. 8, pp. 1462–1474, Aug. 2011.
- [16] C. Zhang, Z. Yuan, Z. Wang *et al.*, “Low complexity sparse Bayesian learning using combined belief propagation and mean field with a stretched factor graph,” *Signal Processing*, vol. 131, pp. 344–349, Feb. 2017.
- [17] Z. Yuan, C. Zhang, Z. Wang *et al.*, “A low complexity OFDM receiver with combined GAMP and MF message passing,” *Telecommun. Syst.*, vol. 71, no. 3, pp. 425–432, Mar 2019.
- [18] J. Ma, X. Yuan, and L. Ping, “Turbo compressed sensing with partial DFT sensing matrix,” *IEEE Signal Process. Lett.*, vol. 22, no. 2, pp. 158–161, Feb. 2015.
- [19] L. Chen, A. Liu, and X. Yuan, “Structured turbo compressed sensing for massive MIMO channel estimation using a Markov prior,” *IEEE Trans. Veh. Technol.*, vol. 67, no. 5, pp. 4635–4639, May. 2018.
- [20] L. Chen and X. Yuan, “Massive MIMO-OFDM channel estimation via structured turbo compressed sensing,” in *Proc. IEEE Int. Conf. Commun. (ICC)*, May 2018, pp. 1–6.
- [21] X. Kuai, L. Chen, X. Yuan, and A. Liu, “Structured turbo compressed sensing for downlink massive MIMO-OFDM channel estimation,” *IEEE Trans. Wireless Commun.*, vol. 18, no. 8, pp. 3813–3826, Aug. 2019.

- [22] J. Winn and C. M. Bishop, "Variational message passing," *J Mach Learn Res*, vol. 6, no. 23, pp. 661–694, Jun. 2005.
- [23] T. P. Minka, "Expectation propagation for approximate Bayesian inference," in *Proceedings of the 17th conference on uncertainty in AI*. Morgan Kaufmann Publishers Inc., Feb. 2001, p. 362–369.
- [24] Z. Yuan, C. Zhang, Z. Wang *et al.*, "An auxiliary variable-aided hybrid message passing approach to joint channel estimation and decoding for MIMO-OFDM," *IEEE Signal Process. Lett.*, vol. 24, no. 1, pp. 12–16, Jan. 2017.
- [25] M.-A. Badiu, G. E. Kirkelund, C. N. Manchón *et al.*, "Message-passing algorithms for channel estimation and decoding using approximate inference," in *Proc. IEEE Int. Symp. Inform. Theory, 2012*, Jul. 2012, pp. 2376–2380.
- [26] D. Zhang, X. Song, W. Wang *et al.*, "Unifying message passing algorithms under the framework of constrained bethe free energy minimization," *IEEE Trans. Wireless Commun.*, vol. 20, no. 7, pp. 4144–4158, Jul. 2021.
- [27] X. Liu, W. Wang, X. Song *et al.*, "Sparse channel estimation via hierarchical hybrid message passing for massive MIMO-OFDM systems," *IEEE Trans. Wireless Commun.*, vol. 20, no. 11, pp. 7118–7134, May 2021.
- [28] J. Cui, Z. Wang, C. Zhang *et al.*, "Localization algorithm based on factor graph and hybrid message passing for wireless networks," *Journal of Computer Applications*, vol. 37, no. 5, p. 1306, May 2017.
- [29] C. Zhang, Z. Yuan, Z. Wang *et al.*, "A new combination of message passing techniques for receiver design in MIMO-OFDM systems," 2017. [Online]. Available: <https://arxiv.org/abs/1701.06304>
- [30] S. Wang, L. Zhou, W. Xu *et al.*, "Hybrid message passing approach for uplink massive MIMO channel estimation," *IEEE Wireless Commun. Lett.*, vol. 11, no. 5, pp. 987–991, Feb. 2022.
- [31] J. Salo, G. D. Galdo, J. Salmi *et al.*, "MATLAB Implementation of the 3GPP Spatial Channel Model (3GPP TR 25.996)," Jan. 2005. [Online]. Available: <http://www.tkk.fi/Units/Radio/scm/>
- [32] M. E. Tipping, "Sparse Bayesian learning and the relevance vector machine," *J Mach Learn Res*, vol. 1, no. 6, pp. 211–244, Jun. 2001.
- [33] N. L. Pedersen, C. N. Manchón, D. Shutin *et al.*, "Application of Bayesian hierarchical prior modeling to sparse channel estimation," in *Proc. IEEE Int. Conf. Commun. (ICC)*, Jun. 2012, pp. 3487–3492.
- [34] Z. Xue, J. Ma, and X. Yuan, "Denosing-based turbo compressed sensing," *IEEE Access*, vol. 5, pp. 7193–7204, May 2017.
- [35] C. R. Berger, Z. Wang, J. Huang *et al.*, "Application of compressive sensing to sparse channel estimation," *IEEE Commun. Mag.*, vol. 48, no. 11, pp. 164–174, Nov. 2010.
- [36] J. P. Vila and P. Schniter, "Expectation-maximization Gaussian-mixture approximate message passing," *IEEE Trans. Signal Process.*, vol. 61, no. 19, pp. 4658–4672, Oct. 2013.
- [37] X. Lin, S. Wu, C. Jiang *et al.*, "Estimation of broadband multiuser millimeter wave massive MIMO-OFDM channels by exploiting their sparse structure," *IEEE Trans. Wireless Commun.*, vol. 17, no. 6, pp. 3959–3973, Jun. 2018.
- [38] J. Kruschke, *Doing Bayesian data analysis: A tutorial with R, JAGS, and Stan*. Academic Press, 2014.
- [39] M. Luo, Q. Guo, M. Jin *et al.*, "Unitary approximate message passing for sparse Bayesian learning," *IEEE Trans. Signal Process.*, vol. 69, pp. 6023–6039, Sep. 2021.
- [40] J. Ma, X. Yuan, and L. Ping, "On the performance of turbo signal recovery with partial DFT sensing matrices," *IEEE Signal Process. Lett.*, vol. 22, no. 10, pp. 1580–1584, Oct. 2015.